



**MARMARA UNIVERSITY**  
**FACULTY OF ENGINEERING**



**INVESTIGATION OF THE PROCESS PARAMETERS  
ON STRAIN INHOMOGENEITY FOR RCS PROCESS**

---

BATUHAN ORAL

**GRADUATION PROJECT REPORT**

Department of Mechanical Engineering

**Supervisor**

Dr. Serkan ÖĞÜT

İSTANBUL, 2023



**MARMARA UNIVERSITY**  
**FACULTY OF ENGINEERING**



Investigation of the Process Parameters on Strain Inhomogeneity for RCS Process

by

**Batuhan Oral**

**08/02/2023- İSTANBUL**

**SUBMITTED TO THE DEPARTMENT OF MECHANICAL ENGINEERING IN  
PARTIAL FULFILLMENT OF THE REQUIREMENTS FOR THE DEGREE  
OF  
BACHELOR OF SCIENCE  
AT  
MARMARA UNIVERSITY**

The author(s) hereby grant(s) to Marmara University permission to reproduce and to distribute publicly paper and electronic copies of this document in whole or in part and declare that the prepared document does not in any way include copying of previous work on the subject or the use of ideas, concepts, words, or structures regarding the subject without appropriate acknowledgement of the source material.

Signature of Author(s) ..... .....

Batuhan ORAL

Department of Mechanical Engineering

Certified By ..... .....  
Res. Asst. Dr. Serkan ÖĞÜT

Project Supervisor, Department of Mechanical Engineering

Accepted By .....  
Head of the Department of Mechanical Engineering

## **ACKNOWLEDGEMENT**

First of all, I would like to thank my supervisor Dr. Serkan ÖĞÜT, for the valuable guidance and advice on preparing this thesis and giving me moral and material support.

February, 2023

Batuhan ORAL

# TABLE OF CONTENTS

<b>ACKNOWLEDGEMENT .....</b>	3
<b>TABLE OF CONTENTS.....</b>	4
<b>ABSTRACT .....</b>	5
<b>SYMBOLS .....</b>	6
<b>ABBREVIATIONS .....</b>	7
<b>LIST OF FIGURES .....</b>	9
<b>LIST OF TABLES .....</b>	11
<b>1. INTRODUCTION .....</b>	12
1.1 Methods of Severe Plastic Deformation.....	13
1.1.1 High Pressure Torsion.....	14
1.1.2 Accumulative Roll Bonding.....	14
1.1.3 Multi Directional Forging .....	15
1.1.4 Twist Extrusion .....	16
1.1.5 Cyclic Extrusion and Compression .....	16
1.1.6 Equal Channel Angular Pressing.....	17
1.1.7 Repetitive Corrugation and Straightening.....	18
1.2 Literature Review .....	19
<b>2. MATERIAL AND METHOD .....</b>	31
2.1 Finite Element Method Analysis.....	31
2.1.1 HPT .....	32
2.1.2 CEC .....	34
2.1.3 ECAP.....	37
2.1.3.1 Incremental ECAP.....	38
2.2 Case Setup .....	39
2.2.1 Determination of Parts .....	39
2.2.2 Drawing of Parts.....	40
2.2.3 Strain Analysis of Parts .....	43
<b>3. RESULTS AND DISCUSSION.....</b>	53
<b>4. CONCLUSION .....</b>	59
<b>5. REFERENCES .....</b>	60

## **ABSTRACT**

### **Investigation of the Process Parameters on Strain Inhomogeneity for RCS Process**

My aim in this project is to obtain Strain values of plastically deformed plates by changing friction coefficient, pressing speed and designing parts at various angles. Thus, we can interpret which criteria affect the Strain value and how. When the graphs we have obtained are examined, it is seen that the friction coefficient and pressing speed do not have a significant effect. When the effect of angle values is examined, it is seen that the Strain Inhomogeneity value generally tends to decrease with increasing angle. However, in some cases, it has been observed that the angle increase has the opposite effect. The most important reason for this is that Strain values are very sensitive to location selection. Friction and print speed have no obvious effect on this graph. However, the value of Strain Inhomogeneity decreases with increasing angle. In other words, a more homogeneous Strain distribution is obtained.

## **SYMBOLS**

**$\alpha$**  :  $R_0/R_1$  ratio

**$\beta$**  :  $r/R_1$  ratio

**$\gamma$**  :  $e/R_1$  ratio

**$\mu$**  : Micron

**$\mu\text{m}$**  : Micrometer

**gf** : Gram-force

**MPa** : Megapascal

**N** : Number of Pass

**nm** : Nanometer

**C** : Celsius degree

**V** : Voltage

**wt%** : Weight percentage

**$\Phi$**  : Channel Angle

**$\Psi$**  : Corner Angle

**$\varepsilon_p$**  : Effective plastic strain

## **ABBREVIATIONS**

<b>Al</b>	: Aluminum
<b>ARB</b>	: Accumulative Roll Bonding
<b>ASTM</b>	: American Society for Testing and Materials
<b>CAD</b>	: Computer-Aided Design
<b>CEC</b>	: Cyclic Extrusion and Compression
<b>CGB</b>	: Constrained Groove Bending
<b>CGP</b>	: Constrained Groove Pressing
<b>CNC</b>	: Computer Numerical Control
<b>CP</b>	: Crack Propagations
<b>Cr</b>	: Chromium
<b>Cu</b>	: Copper
<b>CVHV</b>	: Coefficient of variance of hardness vickers
<b>DI</b>	: Deionized Water
<b>DIN</b>	: Deutsche Institute für Normung (German Institute for Standardization)
<b>ECAP</b>	: Equal Channel Angular Pressing
<b>EDS</b>	: Energy Dispersive X-Ray Spectroscopy-EDS/EDX
<b>Exp.-ECAP</b>	: Expansion Equal Channel Angular Pressing
<b>Fe</b>	: Iron
<b>FEA</b>	: Finite Element Analysis
<b>FWHM</b>	: Full Width at Half Maximum
<b>HPT</b>	: High-Pressure Torsion
<b>HV</b>	: Hardness Vickers
<b>MDF</b>	: Multi-Directional Forging
<b>Mg</b>	: Magnesium
<b>Ni</b>	: Nickel

<b>OM</b>	: optic microscope
<b>SAED</b>	: Selected Area Diffraction
<b>SE</b>	: Standard Error
<b>SEM</b>	: Scanning Electron Microscope
<b>Si</b>	: Silicon
<b>SiC</b>	: Silicon Carbide
<b>SPD</b>	: Severe Plastic Deformation
<b>TE</b>	: Twist Extrusion
<b>TEM</b>	: Transmission Electron Microscope
<b>UTS</b>	: Ultimate Tensile Strength
<b>Zn</b>	: Zinc

## LIST OF FIGURES

<b>Figure 1.1</b> Concept of HPT Tool with material disc placed in the cavity .....	14
<b>Figure 1.2</b> The concept of Accumulative Roll-Bonding where sheets are cut, stacked and rolled.....	15
<b>Figure 1.3</b> Concept showing the setting and pulling along three orthogonal directions .....	15
<b>Figure 1.4</b> The concept of TE shows the shapes of a work-piece before entering, inside the die, and after.....	16
<b>Figure 1.5</b> (a) Cyclic extrusion and compression set up (b) work piece .....	16
<b>Figure 1.6</b> Concept of ECAP (a) Schematic of ECAP facility (b) plane of shear within the die: as indicated in the lower part 1 and 2 numbered element is shear transposed.....	17
<b>Figure 1.7</b> Concept of ECAP showing channel angle $\Phi$ and curve angle $\Psi$ .....	17
<b>Figure 1.8</b> The concept of RCS where the material is corrugated and straightened .....	19
<b>Figure 1.9</b> As-annealed copper has an average grain size of 765 $\mu\text{m}$ .....	20
<b>Figure 1.10</b> (a)–(e) A general morphology of cryomilled Cu with different grain sizes and morphologies. (e) A representative electron diffraction from the nanograins .....	21
<b>Figure 1.11</b> Microstructures in the X, Y, and Z planes and the corresponding SAED in a sample after 18 cycles of RCS process .....	22
<b>Figure 2.1</b> Schematics of ECAP .....	31
<b>Figure 2.2</b> Schematic representation of HPT of thin disks.....	33
<b>Figure 2.3</b> Concept of HPT of bulk disks.....	33
<b>Figure 2.4</b> Microstructure of an aluminium bulk disk subjected to upsetting and torsion[68].....	33
<b>Figure 2.5</b> (a) Equivalent strain distribution after upsetting and (b) after upsetting followed by torsion by $90^\circ$ .....	34
<b>Figure 2.6</b> Schematic representation of HPT of ring.....	35
<b>Figure 2.7</b> Concept of CEC .....	35
<b>Figure 2.8</b> Distribution of equivalent strain after threecycles of CEC [64] .....	35
<b>Figure 2.9</b> Snapshots of die pressure evolution during CEC .....	36
<b>Figure 2.10</b> Equivalent strain distribution for 1.5 and 1 unitoffsets between the input and output passage intwo-turn ECAP with $90^\circ$ [7] (a) and $120^\circ$ (b) angle between channel passages .....	36
<b>Figure 2.11</b> Equivalent strain distribution in two-turn ECAPof a round billet [8] (a) and three-turn ECAP of a square billet (b) established by threedimensional FEM analyses.....	37
<b>Figure 2.12</b> Continuous SPD processes .....	38
<b>Figure 2.13</b> Distribution of equivalent strain for different angle between channel passages, differentsize and shape of the reciprocating die and different direction of the reciprocating move-ment: (a) $90^\circ$ , short flat die, $0^\circ$ ; (b) $110^\circ$ , long flat die, $0^\circ$ ; (c) $90^\circ$ , 1 .....	39
<b>Figure 2.14</b> Sample Piece .....	39
<b>Figure 2.15</b> $30^\circ$ Top Die.....	41
<b>Figure 2.16</b> $30^\circ$ Bottom Die .....	41
<b>Figure 2.17</b> $45^\circ$ Top Die.....	41
<b>Figure 2.18</b> $45^\circ$ Bottom Die .....	42
<b>Figure 2.19</b> $60^\circ$ Top Die.....	42
<b>Figure 2.20</b> $60^\circ$ Bottom Die .....	42
<b>Figure 2.21</b> Workpiece .....	43
<b>Figure 2.22</b> Fix Pattern .....	43
<b>Figure 2.23</b> Generate Mesh .....	43
<b>Figure 2.24</b> Mesh Sheet.....	44
<b>Figure 2.25</b> Determination of Material.....	44

<b>Figure 2.26</b> Determination of Movement.....	45
<b>Figure 2.27</b> Determination of Speed .....	45
<b>Figure 2.28</b> Determination of Friction Coefficient .....	46
<b>Figure 2.29</b> Determination of Stroke.....	46
<b>Figure 2.30</b> First Step .....	47
<b>Figure 2.31</b> Second Step.....	47
<b>Figure 2.32</b> Third Step.....	48
<b>Figure 2.33</b> Forth Step.....	48
<b>Figure 2.34</b> Final Step .....	49
<b>Figure 2.35</b> Strain Regions of the Deformed Part.....	49
<b>Figure 2.36</b> 50 Points of Strain Regions.....	50
<b>Figure 2.37</b> Strain Values of Each Point Can Be Obtained.....	50
<b>Figure 2.38</b> Strain Inhomogeneity Equation .....	51
<b>Figure 2.39</b> Strain Inhomogeneity Index Graph for Pressing Speed of 1 mm/s .....	51
<b>Figure 2.40</b> Strain Inhomogeneity Index Graph for Pressing Speed of 2 mm/s .....	52
<b>Figure 2.41</b> Strain Inhomogeneity Index Graph for Pressing Speed of 3 mm/s .....	52
<b>Figure 3.1</b> Microhardness mapping for the samples processed by (a) 1 pass and (c) 2 passes of heterogeneous RCS and the numerical simulations for passes (b and d).....	54
<b>Figure 3.2</b> Deformation distribution calculated for 1 pass of heterogeneous RCS in the (a) upper and (b) lower faces, (c and d) 2 passes sample of heterogeneous RCS for the upper and lower faces, respectively .....	54
<b>Figure 3.3</b> flow stress of pure aluminium implemented in FEA (see online version for colours)	56
<b>Figure 3.4</b> Strain Inhomogeneity Index Graph for Pressing Speed of 1 mm/s .....	57
<b>Figure 3.5</b> Strain Inhomogeneity Index Graph for Pressing Speed of 2 mm/s .....	57
<b>Figure 3.6</b> Strain Inhomogeneity Index Graph for Pressing Speed of 3 mm/s .....	58

## **LIST OF TABLES**

<b>Table 2.1</b> Results of Strain Inhomogeneity .....	51
<b>Table 3.1</b> Die design parameters used in the present study.....	55

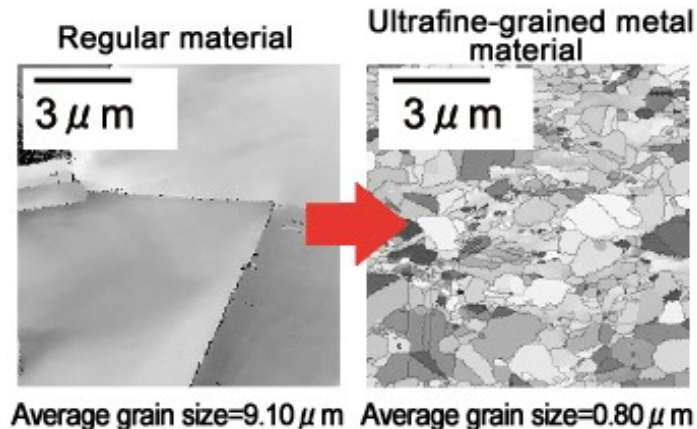
## 1. INTRODUCTION

Recently, the fabrication of metallic alloys with ultra-fine grains (UFG) using severe plastic deformation processes has become an effective way to achieve small grain size in highly deformed metals or alloys. The remarkable strength to weight ratio of the SPD techniques has piqued the interest of some industries, including aerospace and automotive. The Hall-Petch equation states that a large reduction in grain size is beneficial to enhance mechanical characteristics.

Severe plastic deformation (SPD) is a term describing a group of metalworking techniques involving very large stresses, typically involving a complex stress state or high shear, resulting in coaxial ultrafine grain (UFG) size and high defect density. Processes of severe plastic deformation (SPD) are metal forming processes in which a very large plastic strain is imposed on a bulk process in order to create an ultrafine grained metal. A finer grain size increases the strength and the fracture toughness of the material and provides the potential for superplastic deformation at moderate temperatures and high strain rates. Traditional thermo-mechanical processes generally lead to a grain size above  $10\mu\text{m}$  or, exceptionally, a few microns in diameter. However, several techniques to procure submicron or nano-size grains are now available, e.g. vapor deposition, high-energy ball milling, fast solidification and severe plastic deformation (SPD). Processes with severe plastic deformation (SPD) may be determined as metal forming processes in which an ultra-large plastic strain is introduced into a bulk metal in order to create ultra-fine grained metals.

(Korhonen, 2008) [1]

Ultrafine-grained materials are materials with an average grain size refined to around  $1\mu\text{m}$ . Checking the microstructure makes it possible to develop a diversity of properties such as strength and fatigue properties, strength–ductility balance, and workability.

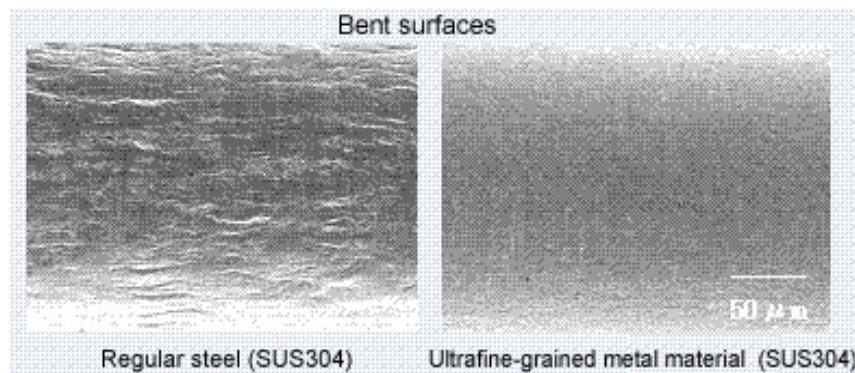


**High strength:** Strength can be raised through severe plastic deformation, which produces an ultrafine elongated grain structure. Increasing strength makes it possible to achieve weight savings by making parts thinner.

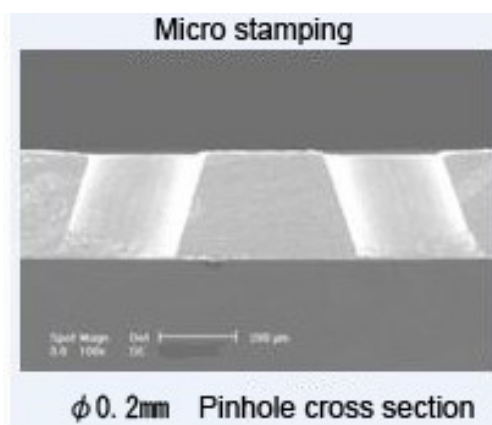
**Improved strength–ductility balance:** Subjecting materials to heat treatment after severe plastic deformation produces an ultrafine equiaxial grain structure that develops strength–ductility

balance. This does it possible to process the metal in a variety of ways without a reduction in strength.

Excellent fatigue properties: Improving fatigue properties does it possible to extend part life.  
Reduction of surface roughness: The ultrafine structure does it possible to reduce surface roughness during metalworking processes (e.g. bending)



Stable sheared surface when pressed: When utilize normal materials with large crystal structures, after pressing, material comes off pressed sections as the product is used. However, with our ultrafine grained steels it is possible to stabilize the contours of micro-sheared surfaces.



The Hall-Petch equation states that a large reduction in grain size is beneficial to enhance mechanical characteristics. For achieving such aim, several techniques of severe plastic deformation have been studied.

### 1.1 Methods of Severe Plastic Deformation

In the recent past several other methods were received for developing ultra-fine grained materials via SPD. The advantage of using SPD is it yields refined grains at very low temperature. The final product thus procured displayes high angled boundaries grains with improved mechanical characteristics. Moreover SPD also yields components with high densification and therefore can be utilized in various automobile, aerospace and defence applications. For the conversion of coarser grains to UFG, it is important to implement a high value of strain so as to obtain highly dense dislocated particles which form an agglomeration at the grain boundaries. SPD produces UFG and thus is defined as a forming technology in which a high value of strain is implemented on a bulk sample without much change in the overall

dimension of the workpieces that also leads to the refinement of grains. Since there is no change in dimensions of components during SPD technique, it can be utilized in very high strain rates. The important severe plastic deformation methods that are already in usage for the production of UFG materials are ARB, MDF, HPT, ECAP, TE, CEC etc. The concept and process of different SPD methods are mentioned in the following sections.

### 1.1.1 High Pressure Torsion

High pressure torsion (HPT) method is considerably more recent method utilized for grain refinement in metal processing, first introduced by Percy Bridgman.

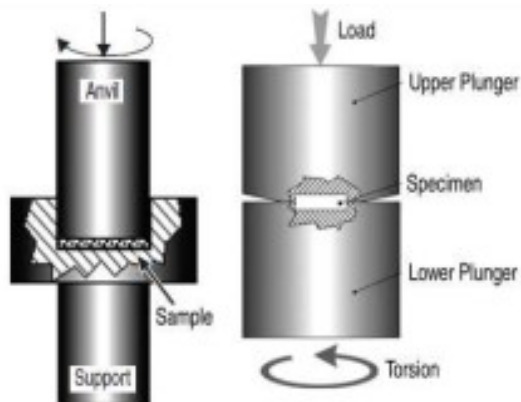


*Figure 1.1 Concept of HPT Tool with material disc placed in the cavity*

Process of this method includes, the material in the form of disc is located between the two anvils, the lower one is known as support anvil and upper one is known as top anvil, and a very large torsional stress in the range of several GPa is applied under high hydrostatic pressure, where the top anvil is rotated to create a torsion force. In this method, the sample in the form of disc may be placed within a cavity of support anvil or in the cavities of both lower support and anvils. Fig.1 shows the concept of HPT where the sample is located within a cavity of the tool, where plastic torsional straining is achieved by rotation of one of the anvils through high hydrostatic pressure.

### 1.1.2 Accumulative Roll Bonding

In this technique, founded in late 90's, the two rolled sheets of the same material are stacked up, heated below the recrystallization temperature, rolled and bonded together to form a single sheet. These sheets are then divided in two halves and then are stacked up, followed by a number of attempts. In comparison to the other technique, this technique proves to be more beneficial as it does not include any specific equipment but only a tool room rolling mill is required. In this technique the two counter parts that are to be joined should be cleaned and mirror polished before rolling so as to give better bonding strength.

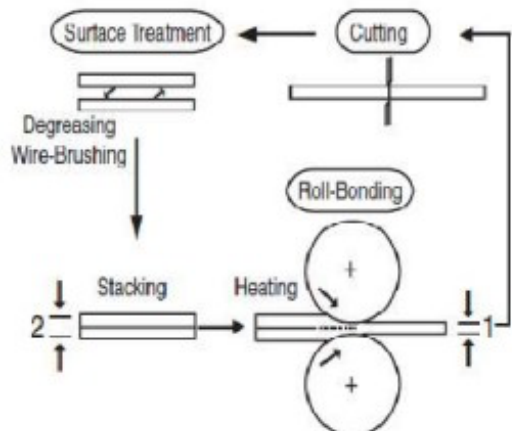


**Figure 1.2** The concept of Accumulative Roll-Bonding where sheets are cut, stacked and rolled

### 1.1.3 Multi Directional Forging

In order to get large strain with less variation in original dimension this technique does use of bulk material. In This technique, continuous setting and drawing is execute in three mutually orthogonal directions. Deformation temperature is an significant factor for the refinement of grains. MDF with high temperature is used for the grain refinement in brittle samples. In earlier study, it was discovered multi axial forging (MAF) on aluminum alloy yields similar properties as compared to ECAP technique. It was also discovered that the values of micro hardness decreased with an increase in values of accumulated strain. However, the homogeneity in strain is improved by MDF is found to be less as compares to ECAP and HPT.

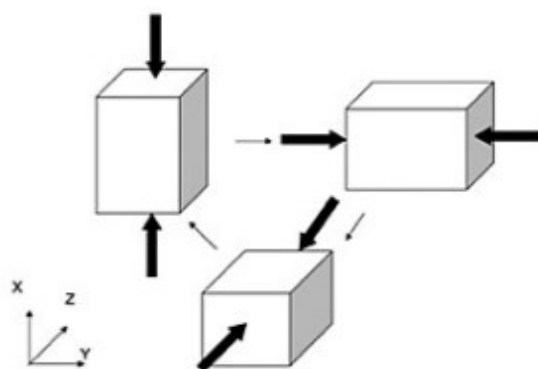


**Figure 1.3** Concept showing the setting and pulling along three orthogonal directions

#### 1.1.4 Twist Extrusion

This is a recent SPD technique. In this, the billet of bulk material created generally in the shape of a square or rectangular rod is allowed to pass through an extrusion die whose dimension will not change when it is twisted through a desired angle along its entire longitudinal axis. It is executed under high values of hydrostatic pressure in the center of deformation. In this method, the sample attains its original dimension after passing through TE technique that allows the repetition of the process several times in order to get superior refinement in grains. By using this technique various cross sectional shapes can be carried out apart from a circular geometry.



**Figure 1.4** The concept of TE shows the shapes of a work-piece before entering, inside the die, and after

#### 1.1.5 Cyclic Extrusion and Compression

CEC technique, also called up as hourglass processing, is one of recently improved technique used for producing ufg and nano materials. In CEC, billet material is thrusted from one chamber to another chamber having equal dimension via a die with a diameter  $d_m = d_0^{0.23}$  which is smaller than  $d_0$ . This technique decreases the grain size of the billet from micrometer to nanometer level. As the name proposes the complete processing is done in two steps, first extrusion followed by second compression

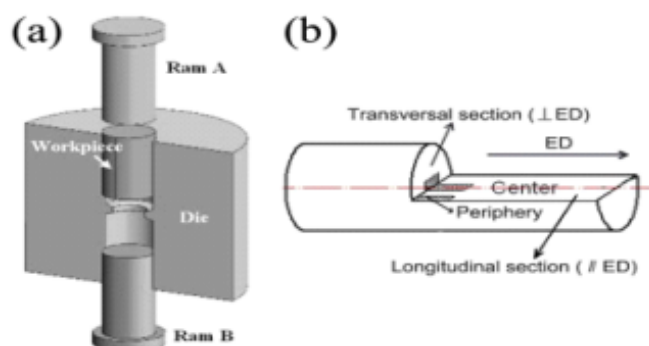


**Figure 1.5** (a) Cyclic extrusion and compression set up (b) work piece

### 1.1.6 Equal Channel Angular Pressing

The ECAP, also identified as equal channel angular extrusion (ECAE), is one of first methods of SPD, was first introduced by Segal and his team members in early 80's at an institute in Minsk in the former Soviet Union. In this process a well lubricated sample of material is compressed by plunger, to pass it through two crossing channels meeting at an oblique angle, which is known as die channel angle  $\Phi$ , in a special die and plastic strain is imposed by simple shear at the intersection of the channels. As the billet passes through the point of intersection point of the two channels a shear strain is introduced. Unlike conventional distortion processes such as rolling , forging, drawing, etc. In this method , as the billet dimensions stay unchanged, the pressing may be repeated , in order to achieve exceptionally high strains with homogeneous equiaxed grains.

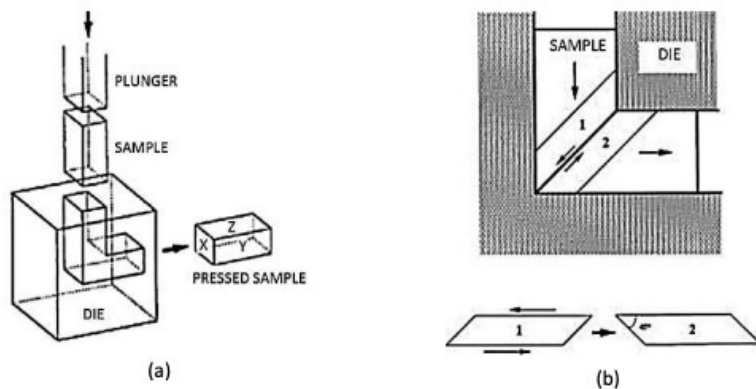


**Figure 1.6** Concept of ECAP (a) Schematic of ECAP facility (b) plane of shear within the die: as indicated in the lower part 1 and 2 numbered element is shear transposed

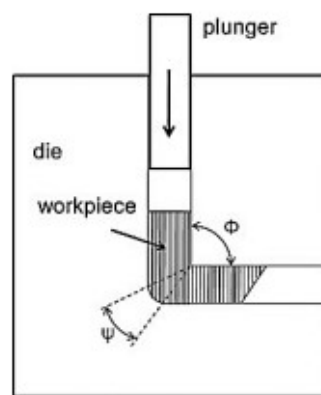


**Figure 1.7** Concept of ECAP showing channel angle  $\Phi$  and curve angle  $\Psi$

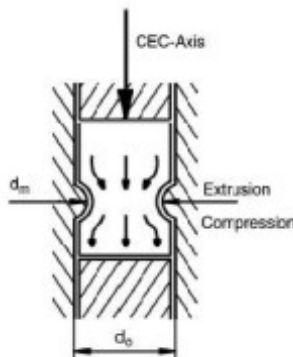
This method exhibits four basic processing carries consisting of different slip systems all through the pressing operation resulting in different microstructures. For grain refinement through ECAP, the billet material is compressed through a special die in which two channels of equal cross-section intersect at channel angle  $\phi$  and corner angle  $Y$ , of the intersection of the two channels. In the frictionless situation between the billets and the die walls, the strain accumulated after  $N$  pressings through the die will be given by the following relationship in equation

*Eq. 1*

$$\epsilon_N = \frac{N}{\sqrt{3}} \left[ 2 \cot \left( \frac{\phi}{2} + \frac{\varphi}{2} \right) + \varphi \cosec \left( \frac{\phi}{2} + \frac{\varphi}{2} \right) \right] (2)$$

During the pressing operation since the cross-section of the compressed billet remains constant after pressing that permits to press the same billet through the die a number of times in order to achieve a high total strain . The above relationships can be directly applied to the center of the billets but not valid at areas away from the center of the billets due to friction .

### 1.1.7 Repetitive Corrugation and Straightening



It is a relatively easy technique of SPD which is utilized for manufacturing of ufg sheets in large quantities. In this technique, the workpiece is deformed to a corrugated form and later on straighten between two parallel plates which imparts high value strain to the samples which leads to refinements of grain, model of continuous RCS can easily be adopted from any manufacturing industry which can yield metallic sheets of fine grains. The RCS facility subjected to both shear and bending, which results grain refinements. Merit of using RCS is that it can easily be used for present industrial rolling technique to yield high amount of fine grained sheets of metals. This technique has strong potential of developing nano structured materials in a continuous and economical manner.

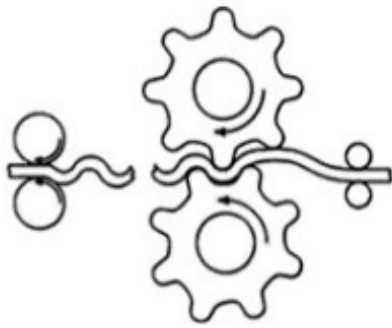


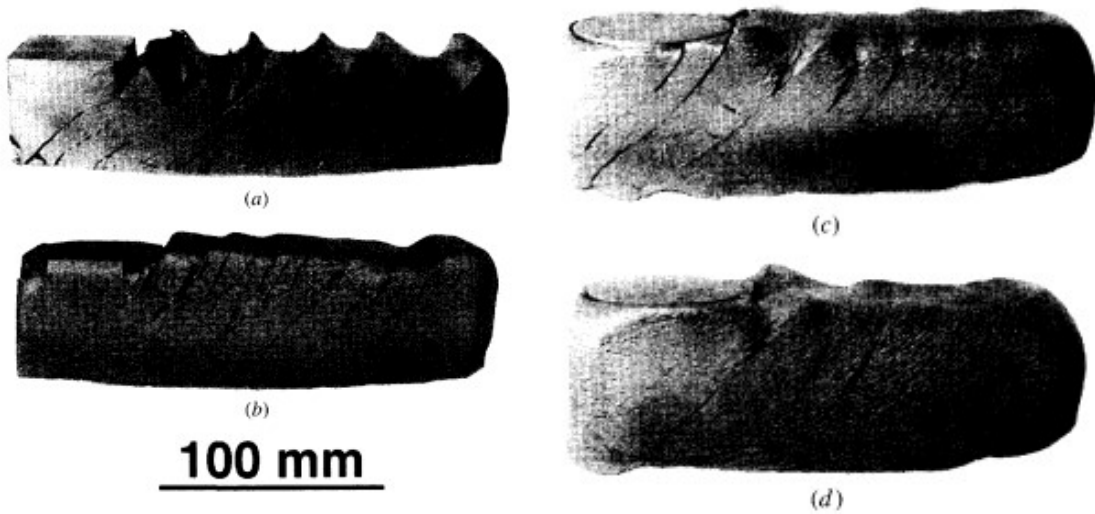
**Figure 1.8** The concept of RCS where the material is corrugated and straightened

Many works have been made for Repetitive Corrugation and Straightening. Various materials were used in these processes. All the works done so far for RCS are listed as follows according to their dates and with which material this process was made. (Segal V ,2018) [2]

## 1.2 Literature Review

There are several studies in literature having similar steps with minor differences. The work was conducted by Zhu Y T, Jiang H. on 01 October 2000. Nanostructured Copper was used as the material. A new process, Repetitive Corrugation and Straightening (RCS), has been improved to create bulk, nanostructured copper. In this investigation, a high purity (99.99%). copper bar measuring 6 x 6 x 50 mm with an average grain size of 765 {micro}m was used as the starting material. It was repetitively corrugated and straightened for 14 times with 90{degree} rotations along its longitudinal axis between consecutive corrugation-straightening cycles. The copper was cooled to below room temperature before each RCS cycle. The grain size obtained after the RCS process was in the range of twenty to a few hundred nanometers, and microhardness was increased by 100%. Both equilibrium and non-equilibrium grain boundaries are observed. This work demonstrates the capability of the RCS process in refining grain size of metal materials. The RCS process can be easily adapted to large-scale industrial production and has the potential to pave the way to large-scale structural applications of nanostructured materials. [3]

The work was conducted by Yuntian T, Lowe,Terry C. on June 2001. Bulk Nanostructured Metals was used as the material. Flow softening when the strain path is replaced after only a small prestrain of the order of 0.10. On the other hand, the results in Figures 1 and 2 reveal that prestrains of the order of 0.20 to 0.40 significantly reduce or essentially eliminate the majority of the flow-softening behavior over intervals of strain comparable to those imposed during one pass through an ECAE die with a 90 deg angle (i.e., a strain of 1.0). Although the changes in strain paths were different in the two cases examined here (plane strain rolling → uniaxial upset vs uniaxial upset → simple shear), it is likely that similar effects and interpretations would pertain for other strain-path changes. Indirect support for this conclusion may be obtained from the work of Korshu- nov et al., 110] who found similar kinetics of dynamic globularization for a variety of deformations involving markedly different types of strain path changes. [4]



The work was conducted by J.Y. Huang, Y.T. Zhu, H. Jiang, T.C. Lowe, on 25 May 2001. Copper was used as the material. The microstructures and dislocation configurations in nanostructured Cu processed by a new technique, repetitive corrugation and straightening (RCS), were learned using transmission electron microscopy (TEM) and high resolution TEM. Most dislocations belong to  $60^\circ$  type and tend to pile up along the  $\{111\}$  slip planes. Microstructural features including low-angle grain boundaries (GBs), high-angle GBs, and equilibrium and non-equilibrium GBs and subgrain boundaries were observed. Dislocation structures at an intermediate deformation strain were studied to investigate the microstructural evolutions, which revealed some unique microstructural features such as isolated dislocation cell (IDC), dislocation tangle zones (DTZs), and uncondensed dislocation walls (UDWs). [5]

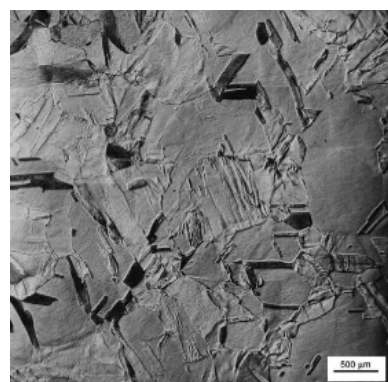


**Figure 1.9** As-annealed copper has an average grain size of  $765 \mu\text{m}$

The work was conducted by JY Huang, XZ Liao, YT Zhu , F Zhou. on 2003. Nanocrystalline was used as the material. The microstructures of cryogenically ball-milled Cu were investigated by high-resolution electron microscopy. It was discovered that the grain-size reduction is a dislocation-controlled continuous process which consists of the formation of small-angle grain boundaries (GBs), a gradual increase in misorientations as a result of accumulation of more dislocations and, finally, the formation of large-angle GBs. The GBs were generally curved, wavy or faceted, and heavily strained, which are typical characteristics of nanostructured materials. In addition, extrinsic dislocations were found in many GBs, indicating that most are in a high-energy non-equilibrium configuration, which is consistent with observations in equal-channel angular pressing processed Cu, Ni, and Al-Mg, repetitive corrugation and straightening processed Cu and roomtemperature ball-milled Cu. These results support a still-disputed concept that GBs in nanostructured metals processed by severe plastic deformation are mostly in non-equilibrium states. [6]

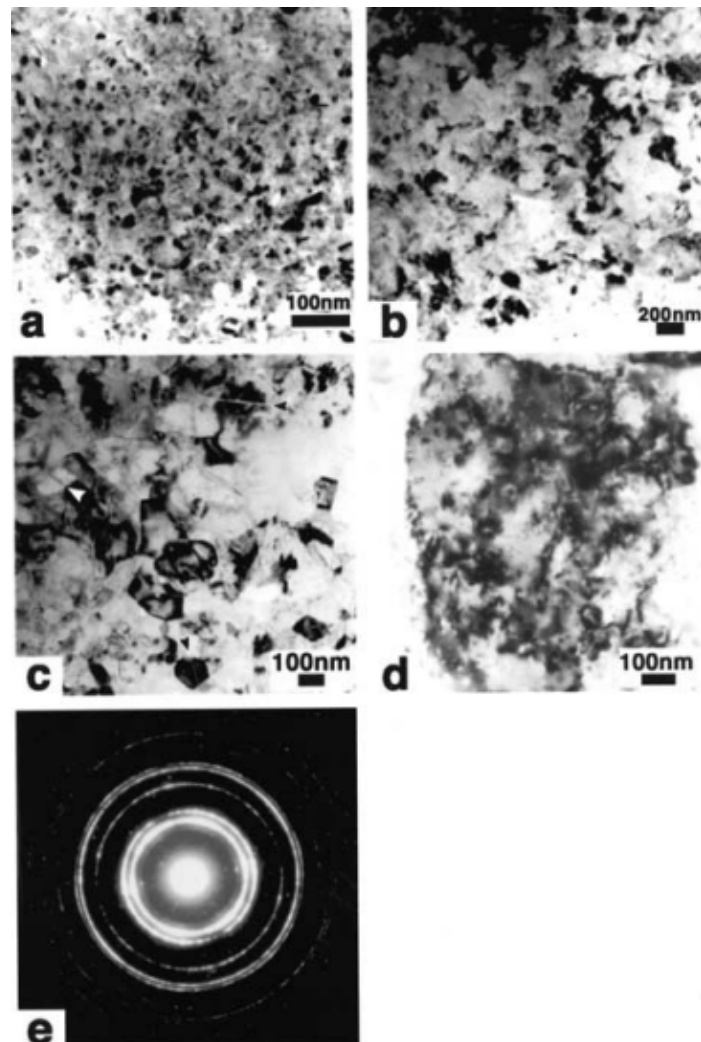


**Figure 1.10** (a)–(e) A general morphology of cryomilled Cu with different grain sizes and morphologies. (e) A representative electron diffraction from the nanograins

The work was conducted by Jianyu Huang, Yuntian T. Zhu, David J. Alexander, Xiaozhou Liao, Terry C. Lowe, Robert J. Asaro. on 25 April 2004. Copper was used as the material. It presents recent improvements in repetitive corrugation and straightening (RCS), a new severe plastic deformation (SPD) technique. Two refinements of the original RCS method are presented and results are shown for commercial purity copper that illustrate the associated improvements in the effectiveness of nanostructuring. Second-generation tooling was implemented using a bench scale rolling mill for continuous processing of sheet and bar. We have found that this design does not produce enough plastic strain per RCS cycle for effective grain refinement prior to the formation and growth of fatigue cracks. Third-generation tooling was designed to process sheet and increase the amount of shear deformation per iteration. The third-generation tooling design introduced significant shear strain and was found to be effective in grain refinement. [7]

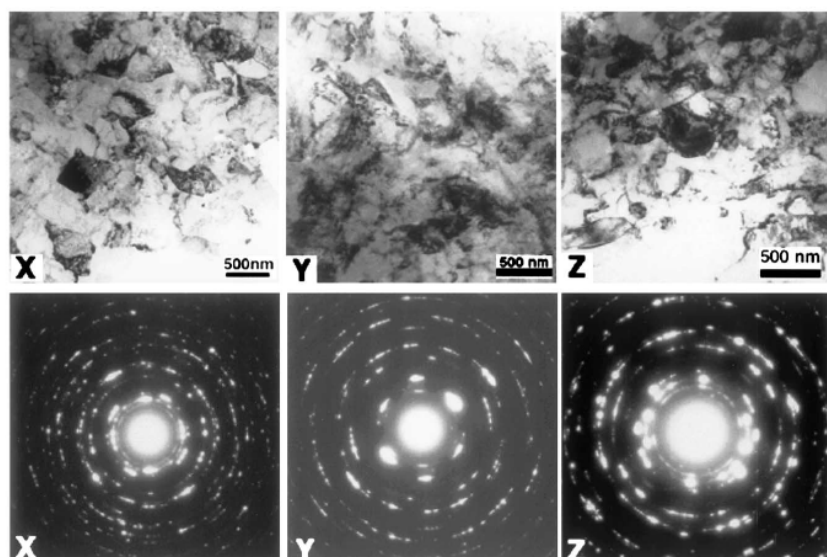


**Figure 1.11** Microstructures in the X, Y, and Z planes and the corresponding SAED in a sample after 18 cycles of RCS process

The work was conducted by V. Rajinikanth, Gaurav Arora, N. Narasaiah, K. Venkateswarlu. on 31 January 2008. Al and Al-0.25Sc alloy was used as the material. The development in strength of Al and Al-0.2Sc alloys through repetitive corrugation and straightening (RCS) was studied. The RCS was carried out using both single teeth as well as multiple teeth corrugative setup attached to a universal testing machine. The improvement in strength was obtained by measuring the hardness after processing. The rotation of sample by 90° between successive passes resulted in higher hardness values as compared to the simple bending and straightening. The increment in hardness obtained with same number of passes in the case of Al-0.2Sc alloy is more as compared to Al and is possibly due to blocking of dislocations that are introduced during deformation by Al<sub>3</sub>Sc precipitates. [8]

The work was conducted by A. Krishnaiah & H. S. Kim. on 15 March 2008. Pure aluminium was used as the material. The feasibility of using the Repetitive Bending and Straightening (RBS) process to develop the mechanical properties of commercial purity aluminium has been investigated. RBS was carried out by bending with a U-bending die of 10 mm radius followed

by straightening between flat dies. The ultimate tensile strength (UTS) and yield strength (YS) slightly increased with increasing number of passes. The maximum UTS of 84 MPa and YS of 68 MPa were obtained after four passes and % elongation to failure decreased from 46% to 35% after four passes. The RBS processed Al showed poor improvement in mechanical properties as compared to other SPD processes. Repetitive bending and straightening process is therefore not an effective process to introduce fine grained structures in metals or alloys. [9]

The work was conducted by Dimitry Orlow on 10 September 2008. Pure Al was used as the material. High purity Al (99.99%) was caused to severe plastic deformation through twist extrusion at room temperature. Microstructures were examined for 1 pass and 4 passes on the cross section perpendicular to the longitudinal axis of billets using optical microscopy and electron back scatter diffraction analysis. It was shown that a vortex-like material flow was observed on the cross section and this became more intense with increasing number of the pressing. After one pass, subgrain structures with low angle grain boundaries were developed throughout the section but after 4 passes, the microstructure consisted of grains surrounded by high angle boundaries with fraction of ~70% in the edge parts. The average grain size at the edge parts is refined to ~1.6 µm. [10]

The work was conducted by J. Stobrawa, Z. Rdzawski , W. Gluchowski , W. Malec. on April 2009. CuCr0.6 alloy was used as the material. Purpose: The aim of this work was to calculate the ability of a continuous repetitive corrugation and straightening (CRCS) technique in creating ultra fine grained copper-chromium strips as well as to determine their deformability, mechanical properties, deformation behaviour and microstructure evolution. Design/methodology/approach: Tests were performed with the 0.8 mm thick CuCr0.6 strips using original die set construction. The changes of mechanical properties as well as microstructure evolution versus number of deformation cycles were investigated. The microstructure was investigated using optical and electron microscopy (TEM and SEM equipped with EBSD). Findings: The obtained strengthening effects and observed microstructure changes have been discussed basing on the existing theories related to strengthening of ultra fine grained copper based materials. The CRCS process effectively reduced the grain size of a CuCr0.6 alloy strips, demonstrating the CRCS as a promising new method for producing ultra fine grained metallic strips. Research limitations/implications: Research results are limited to the initial material after annealing only. Further investigations should be aimed towards determination of CRCS sequence including deformationprecipitation-ageing influence on strengthening effect. Practical implications: A growing trend to use new copper-based functional materials is observed recently world-wide. Within this group of materials particular attention is drawn to those with ultra fine or nanometric grain size of a copper matrix, which exhibit higher mechanical properties than microcrystalline copper. Originality/value: The paper describes to the mechanical properties of precipitates strengthened ultra fine grained copper - chromium alloy strips obtained by original RCS method and to the microstructure evolution. [11]

The work was conducted by Zbigniew Rdzawski, W Gluchowski. on December 2009. CuNi2Si1alloy was used as the material. Purpose: Precipitation strengthened copper constitutes a group of functional and structural materials utilized where combination of high electrical conductivity with high strength is required. A growing trend to use new copperbased functional materials is recently observed world-wide. Within this group of materials particular attention is drawn to those with ultrafine grain size of a copper matrix. Design/methodology/approach: This study was aimed to investigate mechanical properties and microstructure in strips of age hardenable CuNi2Si alloy processed by continuous repetitive corrugation and straightening

(CRCS). Tests were performed with quenched (900°C/1hour/water) or annealed (650°C /1 hour) 0.8 mm thick strips using original die set construction (toothed rolls and plain rolls set) installed in tensile testing machine. The changes of mechanical properties (HV, ultimate tensile strength, 0.2 yield strength) as well as microstructure evolution versus number of deformation cycles were investigated. The microstructure was investigated by optical and electron microscopy (TEM and SEM equipped with EBSD). Findings: The obtained strengthening effects and observed microstructure changes have been discussed basing on the existing theories related to strengthening of ultra fine grained copper based materials. Practical implications: The CRCS process effectively reduced the grain size of CuNi2Si1 alloy strips especially for annealed material, demonstrating the CRCS as a promising new method for producing ultra fine grained metallic strips. Originality/value: The paper contributes to the mechanical properties of precipitation strengthened ultra fine grained copper - chromium alloy strips obtained by original RCS method and to the microstructure evolution. [12]

The work was conducted by J.P. Stobrawa , Z.M. Rdzawski , W. Głuchowski , W. Malec. on 1 December 2009. CuCr0,6 was used as the material. Purpose: The focus of this work was to evaluate the ability of a continuous repetitive corrugation and straightening (CRCS) technique in creating ultra fine grained copperchromium strips as well as to determine their deformability, mechanical properties, deformation behaviour and microstructure evolution. Design/methodology/approach: Tests were performed with the 0.8 mm thick CuCr0.6 strips using original die set construction. The changes of mechanical properties as well as microstructure evolution versus number of deformation cycles were investigated. The microstructure was investigated using optical and electron microscopy (TEM and SEM equipped with EBSD). Findings: The obtained strengthening effects and observed microstructure changes have been discussed basing on the existing theories related to strengthening of ultra fine grained copper based materials. The CRCS process effectively reduced the grain size of a CuCr0.6 alloy strips, demonstrating the CRCS as a promising new method for producing ultra fine grained metallic strips. Research limitations/implications: Research results are limited to the initial material after annealing only. Further investigations should be aimed towards determination of CRCS sequence including deformationprecipitation-ageing influence on strengthening effect. Practical implications: A growing trend to use new copper-based functional materials is observed recently world-wide. Within this group of materials particular attention is drawn to those with ultra fine or nanometric grain size of a copper matrix, which exhibit higher mechanical properties than microcrystalline copper. Originality/value: The paper describes to the mechanical properties of precipitates strengthened ultra fine grained copper - chromium alloy strips obtained by original RCS method and to the microstructure evolution. [13]

The work was conducted by H. Sheikh. on 12 March 2010. Duratherm 600 cobalt superalloy was used as the material. The effect of repetitive corrugation and straightening (RCS) process on hardness of Duratherm 600 superalloy has been investigated. To do so, the RCS was carried out until 25 cycles using multiple teeth corrugative setup that the rotation of sample with 90° between cycles was utilized. The results show that the increasing of cycle number enhances the value of hardness. Also, the microstructures of samples are an evidence of slipbands formation during RCS showing the applied strain on the material. As a result, the increasing of hardness can be attributed to formation of subgrains, LAGBs and hcp martensitic plates at large strains. [14]

The work was conducted by F. Khodabakhshi, M. Kazeminezhad, A.H. Kokabi. on 25 June 2010. Low carbon steel was used as the material. A severe plastic deformation method called constrained groove pressing (CGP) is used for imposing a high magnitude of strain into the low carbon steel sheets. Microstructural changes during process are examined by X-ray diffraction and optical observations. The grain size evolution during severe plastic deformation is studied using Williamson–Hall analysis on XRD pattern of the deformed samples. In effective strain of 4.64, ferrite grains with a submicron size of 200–300 nm are achieved. The results show that constrained groove pressing can effectively refine the coarse-grained structure to an ultra fine grain range. Mechanical properties changes due to microstructure evolution are measured by tensile and hardness tests. The results show that the constrained groove pressing process leads to decrease of work hardening rate and increase of strain rate sensitivity of the sheets material. Finally, in cumulative strain of 4.64, a deformed sheet with grain size of 230 nm and ultimate tensile strength of 400 MPa is obtained. [15]

The work was conducted by J. Stobrawa, Z. Rdzawski. on 2011. Precipitation hardened copper alloys were used as the material. Precipitation strengthened copper belongs to a group of functional and structural materials applied where combination of high electrical conductivity with high strength is required. A growing trend to use the new copper-based functional materials is observed recently worldwide. Within this group of materials particular attention is drawn to those with ultrafine grain size of a copper matrix. This study was aimed to investigate mechanical properties and microstructure in strips of age-hardenable copper alloys processed by continuous repetitive corrugation and straightening (CRCS). Tests were performed on 0.8 mm thick, CuCr0.6 and CuNi2Si1 alloys strips annealed at 650°C for 1 hour. The specially designed construction of die set (toothed rolls and plain rolls set) installed on tensile testing machine was applied for deformation process. The changes of mechanical properties (HV, ultimate tensile strength, 0,2 yield strength) as well as microstructure evolution versus number of deformation cycles were studied. The microstructure was observed with optical and electron microscopes (TEM and SEM equipped with EBSD). The CRCS process effectively reduced the grain size of CuCr0.6 and CuNi2Si1 alloys strips, demonstrating the CRCS as a promising new method for producing ultra-fine grained metallic strips. [16]

The work was conducted by S.C. Pandey, M.A. Joseph,M.S. Pradeep,K. Raghavendra,V.R. Ranganath,K. Venkateswarlu, Terence G. Langdon. on 1 February 2012. Al-Cu and Al-Sc alloys were used as the material. Two alloys of Al–Cu and Al–Cu–Sc were processed for up to 4 passes using a facility for continuous repetitive corrugation and straightening (RCS). Hardness measurements were taken on the processed samples and specimens were cut from the processed sheets and tested in tension at room temperature. The results demonstrate that processing by RCS gives a very significant increase in hardness and this high level of hardness is introduced throughout the length of each sample. Thus, there is no wastage when metals are processed by RCS. The hardness values are further increased, and the degree of homogeneity is improved, if the samples are rotated by 90° between each consecutive pass through the RCS facility. The strength is higher for the Al–Cu–Sc alloy than for the Al–Cu alloy. A theoretical model is developed to explain the strength developed during processing by RCS. It is shown by calculation that the theoretical model is in excellent agreement with the experimental results. [17]

The work was conducted by Susheelkumar Vijapur, M Krishna, H N Narasimha Murthy. on 4 August 2012. Al sheets were used as the material. The aim of the work was to study the effect of number of cycles on hardness and tensile strength of Al sheet materials processed by corrugative and straightening method. Al sheets were processed for up to 30 cycles using

specially designed and developed geared corrugation and roller straightening setup. The microstructure, tensile and hardness studies were done as per standard methods. The microstructural study showed that finer grain refinement seen at 20th cycle then it grain dissolution could be seen. The experimental result showed that the hardness and tensile strength increasing with increase in number of cycles and reach maximum (105 Hv and 405 Mpa) at 21st cycle then they decreased due to grain dissolution. [18]

The work was conducted by Arya Mirsepasi,Mahmoud, Nili-Ahmabadabi,Mohammad Habibi-Parsa,Hadi Ghasemi-Nanesa,Ahmad F. Dizaji. on 15 August 2012. Martensitic steel was used as the material. The method of severe plastic deformation (SPD) is often used to produce bulk ultrafine grained (UFG) metallic materials. SPD is a procedure, whereby the initial coarse grained structure of the material usually changes to deformed and UFG state. In the present study, a new SPD process called repetitive corrugation and straightening by rolling (RCSR) is introduced. A strain calculation method is then reported for inducing high strains after repetitive cycles in order to fabricate UFG metallic materials. RCSR consists of corrugated and flattened rolls. Changeable position of the workpieces during different routes, is of substantial capabilities of this procedure. Fe–10Ni–7Mn martensitic steel sheets were subjected to RCSR process. Optical and scanning electron microscopy along with mechanical testing investigation was used to systematically study the microstructure and mechanical properties of the workpieces. Microstructural study depicts micro-voids formation with average size of 100–150 nm. The spherical morphology appeared mostly along the laths, resulted from the nonequilibrium grain boundaries. [19]

The work was conducted by H. S. Siddesha on 18 October 2012. Aluminum was used as the material. The severe plastic deformation process is capable of developing the submicron grain structures in metallic alloys and to improve the mechanical properties. Repetitive corrugation and straightening (RCS) processes are widely used in industries to compensate the highstrength metal plates components used in automobiles. In this work, an attempt has been made to study the influence of RCS parameters like strain rate, number of passes, and plate thickness to produce grain refinement in metallic alloys. Experiments were based on the Taguchi method and the analysis of variance (ANOVA) technique was an effective tool to predict the degree of importance of the RCS parameters on grain size, microhardness, and tensile strength of RCS specimens. The results indicated that the number of passes has a major influence on the fine grain refinement, followed by Al plate thickness and strain rate. [20]

The work was conducted by W. Kwaśny , P. Nuckowski , Z. Rdzawski , W. Głuchowski. August 2013. CuSn6 alloy was used as the material. Purpose: The goal of the study is try to find the influence of plastic deformation using the RCS (repetitive corrugation and straightening) process on the structure and mechanical properties of CuSn6 alloy. The influence of process parameters on the above property were investigated. Obtained results were correlated with the results obtained for alloy subjected to cold rolling. Design/methodology/approach: This study was aimed to investigate structure and mechanical properties non annealed strip of CuSn6 alloy, cold-rolled and the tape subjected to intensive plastic deformation using the RCS method (repetitive corrugation and straightening). Findings: Research have shown increase compressive stresses and tensile strength in material after RCS process compared to classic rolled. Crystallite size measurement confirmed the presence of nanoscale structures in the studied materials after deformation by RCS process. The used method of plastic deformation is promising for development materials with improved properties. Research limitations/implications: The research was carried out on samples, not on final elements. Practical implications: Research is moving towards the development of the materials with finest

microstructure, known as ultra-fine-grained materials with improved properties, compared to currently known materials. Originality/value: This paper presents the results of study of the structure and mechanical properties CuSn6 alloy deformed in the RCS (repetitive corrugation and straightening) process. [21]

The work was conducted by F. Khodabakhshi, M. Abbaszadeh, H. Eskandari, S.R. Mohebpour on October 2013. Steel sheets was used as the material. A modified method of severe plastic deformation (SPD) entitled constrained groove pressing-cross route (CGP-CR) was introduced for imposing a high magnitude of equivalent strain of about 2.32 per pass on the sheet form samples. The major benefit of this improved route compared to previous common route was the more homogeneity of strain in the rolling (RD) and transverse (TD) directions of sheets. In this study, low carbon steel samples were used for examination of evolutions in microstructure and mechanical properties during SPD via CGP-CR process. Mechanical properties improvement were measured by tensile and macro hardness tests. The results indicate that CGP-CR process can effectively improve tensile strength; and also, yield stress and hardness of as-received low carbon steel samples were improved up to about 100% after two deformation passes. Also, high magnitude of inhomogeneity can be observed in hardness distribution through first pass of the process which diminishes in the subsequent passes. Microstructural evolutions during process were monitored by optical microscopy observations and X-ray diffraction analysis. The results demonstrate that initial ferritic microstructure with grain size of about 30  $\mu\text{m}$  was refined to a 225 nm cell structure after two passes of CGP-CR process. [22]

The work was conducted by Sunil, B. Ratna. on 16 October 2014. Steel sheets was used as the material. Recently, severe plastic deformation (SPD) techniques have been gaining wide popularity in developing nano/ultrafine grained (UFG) structured materials for a wide variety of applications. Among SPD techniques, there are a few techniques that are specially used to process metallic sheets and plates. Repetitive corrugation and straightening (RCS) is one such promising technique, which can produce fine grained structures in metallic sheets or plates in bulk. The process was introduced to develop UFG metallic sheets and plates nearly a decade ago and is now gaining great interest in the material processing field. The aim of the present review is to give a comprehensive summary of the state-of-the-art of the process in developing fine grained structured sheets. Emphasis has been given to discuss different material systems processed by RCS. The mechanism behind the grain refinement during RCS, promising applications, and future perspectives in developing UFG structured sheets or plates by RCS are also discussed. [23]

The work was conducted by N. Thangapandian, S. Balasivanandha Prabu. on 23 July 2015. Aluminum Alloy (AA 5083) was used as the material. The microstructure and mechanical properties of aluminium alloy (AA 5083) processed through Repetitive Corrugation and Straightening (RCS) was studied. The RCS process consists of corrugating a flat specimen with a pair of systematically grooved dies and straightening was done with two parallel flat dies. The aluminium samples were subjected to RCS process using two different die: Die I-semi grooved die with breath = height = 5 mm and  $\theta = 30^\circ$  and Die II-semicircular profile with radius = 10 mm. The specimens were subjected to maximum 8 passes for die I but the other one went upto 14 pass. The grain refinement was studied from the microstructure examination using TEM. The mechanical properties such as tensile strength, hardness and the grain size were compared. The tensile strength and hardness were found increasing with respect to the number of passes. The tensile strength increased 25% in the sixth pass when compared to the parent material. But the

strength and hardness values were reduced at 8th pass due to the surface cracks. The TEM studies showed that the Die-I is superior to Die-II in terms of grain refinement. [24]

The work was conducted by Peyman Asghari Rad , Hassan Shirazi , Sebastian Koldorf, Mahmoud Nili-Ahmabadi. on 12 November 2015. Austenitic Stainless Steel was used as the material. The present paper describes the effect of sever plastic deformation on the microstructure and mechanical properties of AISI type 304 stainless steel deforemd by the repetitive corrugation and straightening by rolling (RCSR) at 0°C. A thermomechanical treatment based on the reversion of strain-induced martensite was employed to produce fine-grained structure in a 304 stainless steel. The strain-induced martensite phase increased with increasing of strain up to 90% for 30-cycle of RCSR specimen. Nucleation of  $\alpha$ -martensite observed at the intersections of deformation bands, preferentially at intersections of two  $\varepsilon$  -bands and following  $\gamma \rightarrow \varepsilon \rightarrow \alpha$  sequence. X-ray diffraction was used to identify the strain-induced martensite phase and its volume fraction. Micro hardness of specimens has increased with increasing of RCSR cycles due to formation of mechanical twins and martensitic transformation. [25]

The work was conducted by Prabhakar M Bhovi ,K. Venkateswarlu. on 14 November 2015. Al-3Mg and Al-3Mg-0.25Sc alloys was used as the material. A comparative study was conducted to evaluate the influence of two different severe plastic deformation (SPD) processes: repetitive corrugation and straightening (RCS) and high-pressure torsion (HPT). Samples of an Al-3Mg-0.25Sc alloy with an initial grain size of  $\sim 150$   $\mu\text{m}$  were processed by RCS through 8 passes at room temperature either without any rotation during processing or with a rotation of 90° around the longitudinal axis between each pass. Thin discs of the alloy were also processed for up to 5 turns by HPT at room temperature. The results show that both procedures introduce significant grain refinement with average grain sizes of  $\sim 0.6\text{--}0.7$   $\mu\text{m}$  after RCS and  $\sim 95$  nm after HPT. Measurements of the Vickers microhardness gave values of  $\sim 128$  after RCS and  $\sim 156$  after HPT. The results demonstrate that processing by HPT is the optimum processing technique in achieving both high strength and microstructural homogeneity. [26]

The work was conducted by N. Thangapandian,S. Balasivanandha Prabu,K.A. Padmanabhan. on 1 January 2016. Al-Mg alloy was used as the material. It is shown that a proper selection of corrugation die profile and die parameters is essential for achieving homogeneous grain refinement in materials subjected to repetitive corrugation and straightening (RCS). An Al-Mg (AA 5083) alloy was subjected to the RCS process using three different corrugation die profiles (V-groove, Flat groove, and Semi-circular groove), followed by straightening to determine the allowable maximum number of passes prior to surface cracking/fracture. Mechanical properties, i.e., hardness and tensile strength of the RCS samples were measured and compared as functions of corrugation die profiles and number of passes and the changes in microstructure. Grain refinement was studied using Electron Back Scattered Diffraction (EBSD) analysis and Transmission Electron Microscopy (TEM). [27]

The work was conducted by N. Thangapandian, S. Balasivanandha Prabu & K. A. Padmanabhan. on 17 January 2016. AA5083 Aluminum Alloy was used as the material. Repetitive corrugation and straightening experiments were carried out on sheets of aluminum alloy, AA5083, at room temperature and 573 K (300 °C) and two pressing velocities (0.5 and 2 mm/s). In every case, the sheet was processed to the maximum possible number of passes. Electron backscattered diffraction analysis and transmission electron microscopy were used to characterize microstructure evolution. After room temperature processing with a pressing velocity of 0.5 mm/s, the average grain size had decreased to  $\sim 11$  microns from  $\sim 45$  microns,

with 70 pct of the grain boundaries of the high-angle type. In contrast, sub-grain formation was present at a pressing velocity of 2 mm/s. Mechanical properties like tensile strength and hardness were correlated with microstructures. It is concluded that the velocity of pressing plays a crucial role in grain refinement and recovery and the resulting mechanical properties, as the time available for dislocation rearrangements during processing depends strongly on this variable. An increase in temperature of deformation leads to softening and a deterioration in the mechanical properties. [28]

The work was conducted by Mahmoud Nili-Ahmabadi , Hassan Shirazi. on 12 May 2016. A356 Aluminum Alloy was used as the material. Semi-solid metal forming is a new developing technology that has some advantages in relation to other forming and casting techniques. This process contains three main steps; feedstock manufacturing, reheating and forming. In this study, in order to produce highly strain feedstock from A356 aluminum alloy, a new severe plastic deformation method named repetitive corrugation and straightening by rolling (RCSR) is utilized. RCSR process including corrugated and flattened rollers acquires accumulative strain in material with minimum dimensional changes. A356 alloy specimens were subjected by RCSR process for various numbers of cycles to investigate the effect of strain on the morphology and shape factor of reheated specimens. Moreover, effect of holding temperature and time were on microstructure change were investigated. According to the microstructure observations, with increasing the number of RCSR cycles, besides decreasing in spherical size of particles, sphericity was increased and took place in less reheating time. Results indicate that RCSR process followed by reheating was effective to produce plate shape material with fine globular microstructure. [29]

The work was conducted by Prabhakar M. Bhovi,Deepak C. Patil,S.A. Kori,K. Venkateswarlu,Yi Huang,Terence G. Langdon. on October–December 2016. Al-Mg-Sc alloy was used as the material. The computer aided design (CAD) model of corrugated and straightened dies in repetitive corrugation and straightening (RCS) process used in this study. RCS is one of the promising techniques among various severe plastic deformation (SPD) methods. The Al-Mg-Sc alloy was processed up to four passes; each pass consists of corrugation and straightening. The sample was subjected to RCS and a finite element analysis was carried out for prediction of field parameters such as effective strain and deformation rate. These parameters were analyzed up to four passes of RCS process using advanced tool AFDEX-2014. The obtained value of effective strain was in good confirmation with experimental results. It is essential to know the effective strain induced in the sample during processing of Al-Mg-Sc alloy. Simulation work for flow pattern of effective strain and deformation rate of the sample was studied. The large plastic strain imparted in the material after RCS lead to grain refinement, produced ultrafine grained structure and subsequently improved hardness value of 118 VHN in Al-Mg-Sc alloy after four passes, as compared to 45 VHN for as cast alloy. [30]

The work was conducted by N. Thangapandian , S. Balasivanandha Prabu. on December 2016. Al-Mg-Si Aluminium Alloy was used as the material. Repetitive Corrugation and Straightening (RCS), a promising Severe Plastic Deformation technique (SPD) is used to produce ultrafine grained (UFG) / nanostructured material in coarse grained structure. In this work, Al-Mg-Si aluminium alloy was subjected to RCS process at two different pressing speeds (0.5 and 2.0 mm. Sec<sup>-1</sup>) with the RCS die having equal breadth and height of 5 mm and the groove angle ( $\theta$ ) of 30°. The specimens were processed to the maximum of 8 numbers of passes. The microstructural features were studied using TEM. TEM micrographs confirm the formation of dislocation cell in Al-Mg-Si alloy after 8 pass at room temperature processing condition. The sub-grain formation related to the strength. Tensile strength and hardness of the RCSed

specimen were studied and compared in order to study the effect of pressing speed on the properties. The strength and hardness were high in the specimen prepared at low pressing speed. The hardness value increased to 86 HV and 96 HV at the end of 8 passes respectively for 1 mm. sec-1 and 0.5 mm. sec-1 respectively, originally form 69 HV. The strength increases in a linear manner with the increase in number of passes. The strength increased to 187 MPa at the end of 2 pass processed with the pressing speed of 0.5 mm. sec-1 and 178 MPa at the end of 6th pass processed with the pressing speed of 2 mm. sec-1. The unprocessed alloy shows 70 MPa as strength. [31]

## 2. MATERIAL AND METHOD

In this section of the thesis, the materials and the methods used within the thesis were clearly described. Finite Element Analysis numerical examples were described within material and method.

### 2.1 Finite Element Method Analysis

Severe plastic deformation (SPD) is a method of converting coarse grained metals into ultrafine grained metals, which possess improved mechanical and physical properties. However, none of the many proposed SPD processes have, as yet, gained a commercial acceptance. The finite element method (FEM) is an invaluable tool, which can help to understand the mechanics of material flow in order to optimize existing SPD processes and develop new SPD processes. This reviews the literature on FEM simulation of the most popular SPD process of equal channel angular pressing (ECAP) and presents a number of case studies based on FEM analyses of some other SPD processes.

The first finite element method (FEM) simulation of ECAP was performed in 1997 [32]. As many future simulations, it assumed a two-dimensional plane strain model and investigated the effect of channel geometry and friction on the plastic flow of the material. Interestingly, the tools were modelled as elastic bodies an approach which has not been tried again since then. Another early FEM analysis of ECAP also evaluated the effect of friction but, more importantly, it dealt with a hot process [33]. The analysis took into account heat generation and heat transfer during ECAP as well as the temperature and strain rate sensitivity of the processed material. The simulations described in reference [33] were performed for both two dimensional and three dimensional models.

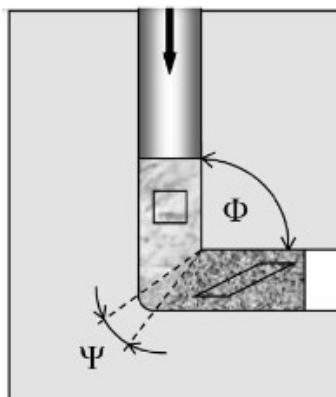


Figure 12.1 Schematics of ECAP

The vast majority of FEM simulations that followed these early publications were carried out with a view to assess the influence of the tool geometry, process conditions, and materials properties on strain homogeneity of the ECAP billets and, less frequently, to assess the process force. As shown in Fig. 12, the channel geometry could be varied by using different values of the channel angle  $f$  [34, 35], or the outer corner angle  $\Psi$  [36–41], or both [42–44]. The width of the input channel could be made different from that of the exit channel (thus deviating from pure ECAP) [45]. A radical change in the channel geometry was the addition of more channel turns

either in the U-shape or S-shape configuration [34–37,45–48]. The main factors describing ECAP conditions were friction [37–39,41,44,46,49–52] and, less frequently, back pressure [36,41,43,50]. The tool temperature was considered rarely [41,46,53]. In references [53] and [54], a slightly different approach, known as a finite volume method, was adopted. The prevailing material model used was based on strain hardening. Only few authors disregarded it and assumed perfect plasticity [42,45,52]. In some cases, the perfect plastic model was added as a limiting condition for strain hardening [47,50] or as a model to be compared with strain hardening [38,44,51,55,56]. Two different strain hardening curves for reversed loading (taking place for 180° billet rotation between consecutive passes of ECAP) were used in reference [57]. The effect of strain softening was analysed in reference [51]. Strain localization and tensile stresses lead to fracture, which was simulated in references [33], [51], and [58]. Strain rate sensitive material models were reconsidered in references [21], [26], [30], [51], [53], [54], and [59]. Gurson porous material model was used in reference [60]. The attempts to use models with microstructure together with FEM analysis are rare. In reference [56], strain distribution results were used to obtain the textures developed during ECAP. A dislocation-based strain hardening model was implemented in a finite element code which enabled cell size evolution to be predicted [61]. Although stress and reaction forces are routinely available from FEM simulations, only few papers mentioned these results and used them to evaluate material behaviour, tool pressure, and the process force [36–38,53,59]. The vast majority of ECAP simulations used a two-dimensional model assuming plane strain. For round billets and rectangular billets with friction and heat transfer, three-dimensional simulation is more appropriate, as shown in references [37], [46], [52] to [54], [62], and [63]. All mentioned so far referred to ECAP. There were only a few FEM simulations of other SPD processes. One of them was reference [64], where cyclic extrusion compression (CEC) was analysed. High pressure torsion (HPT) of thin disks was considered in reference [65] whereas constrained groove pressing and constrained groove rolling were simulated in reference [66].

The present will show how FEM analysis can be used to help assess technical feasibility of the existing SPD processes and develop new SPD processes. For those who are unfamiliar with the concept of UFG metals made by SPD, the second chapter will introduce the subject. The third chapter will present a few case studies of batch SPD processes such as HPT, CEC, and a multi-turn ECAP. The fourth chapter will cover a new continuous SPD process called incremental ECAP (I-ECAP). The closing remarks will summarize the authors' view on the usefulness of FEM analysis in developing practical SPD processes.

### 2.1.1 HPT

A standard torsion test terminates quickly due to fracture caused by limited ductility of metals. In order to suppress fracture, high pressure is superimposed onto torsion [67]. However, HPT, which is one of the popular laboratory SPD processes, has many disadvantages. These are: small and thin specimens, non-uniform strain along the specimen radius and a very high pressure required to transfer the torque by friction (about 5–6 GPa). An attempt was made to replace thin disks with bulk disks as shown in Fig. 14 [68].

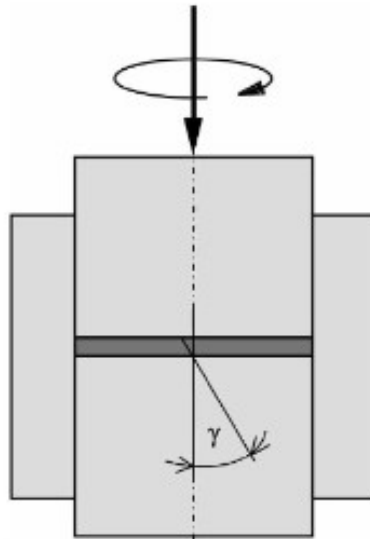


**Figure 2.2** Schematic representation of HPT of thin disks

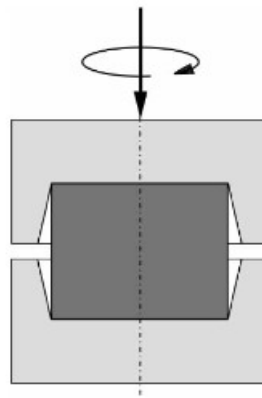


**Figure 2.3** Concept of HPT of bulk disks

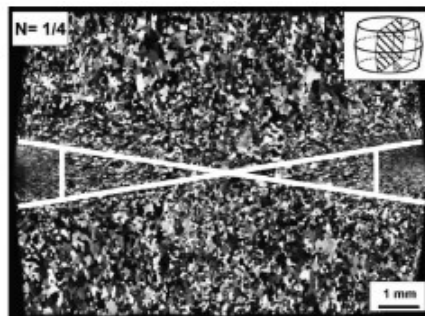


**Figure 2.4** Microstructure of an aluminium bulk disk subjected to upsetting and torsion[68]

The process involved upsetting the billet in order to fill the conical dies to provide large tool contact area and then rotating one of the dies to cause torsional deformation in the billet. As illustrated in Fig. 15, the grain structure resulting from 1/4 rotation of the die was very inhomogeneous. The UFG zones were localized in the outer area of the middle plane. The FEM equivalent strain results presented in Fig. 11 confirm these experimental findings; the

superposition of non-uniform strain caused by upsetting and non-uniform strain resulting from torsion produces maximum strain in the same area in which the UFG zones are observed. Another configuration of HPT, introduced in the 1970s [69], uses a ring rather than a disk (Fig. 12). Comparing the ring configuration in Fig. 12 with the UFG zones marked by the white lines in Fig. 10, an analogy can be seen. Due to uniform strain, HPT of rings enables better utilization of the material. The process requires lower pressure to transfer the torque (due to a ribbed compression tool) and can be scaled up to produce large rings. The rings can be cut and straightened to obtain straight bars. In the opinion of the authors, HPT of rings, which has been forgotten for many years, deserves a second chance as a viable SPD process.

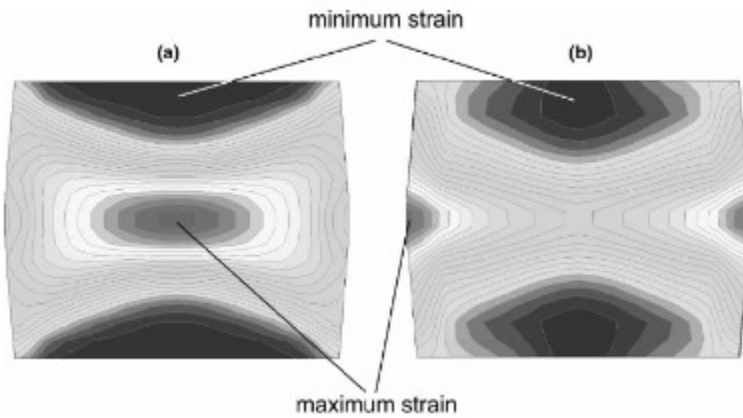


*Figure 2.5 (a) Equivalent strain distribution after upsetting and (b) after upsetting followed by torsion by 90°*

### 2.1.2 CEC

CEC is a well established SPD process, used mainly in Poland, where it was invented in the 1980s [61]. It is based on the application of a counter-pressure which is high enough to cause plastic compression of the extruded billet (Fig. 18). To accumulate large plastic strain, the process is repeated by moving the material cyclically between the two die chambers. The process was developed without a detailed knowledge of the stress/strain state generated in the material. Only later, an FEM analysis provided a better insight into such details [64]. It revealed surprisingly uniform strain distribution in the middle part of the billet but also extensive end effects (Fig. 19). This means that the longer the billet the better material utilization.

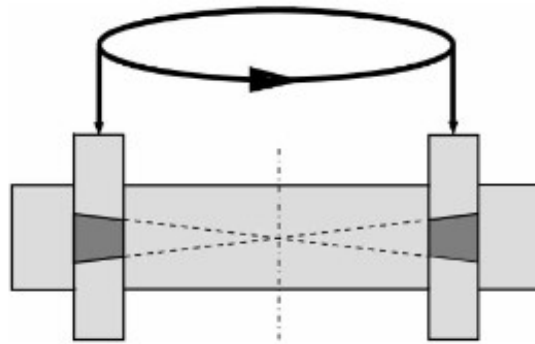


**Figure 2.6** Schematic representation of HPT of ring

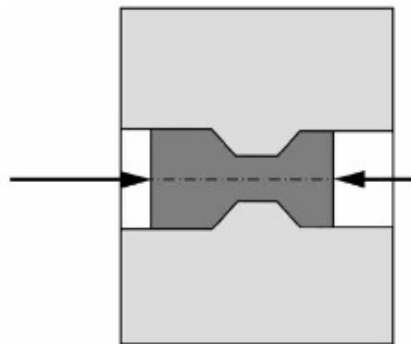


**Figure 2.7** Concept of CEC



**Figure 2.8** Distribution of equivalent strain after three cycles of CEC [64]

On the other hand, the forward extrusion force is known to be very sensitive to the billet length because of friction. Therefore, to avoid an excessive punch and die stress, the maximum billet length has to be limited. The maximum tool pressure in CEC is higher compared with forward extrusion because of a counter-force applied on the compression side. For the same reason, the tool pressure change during CEC is different from that normally observed in forward extrusion.

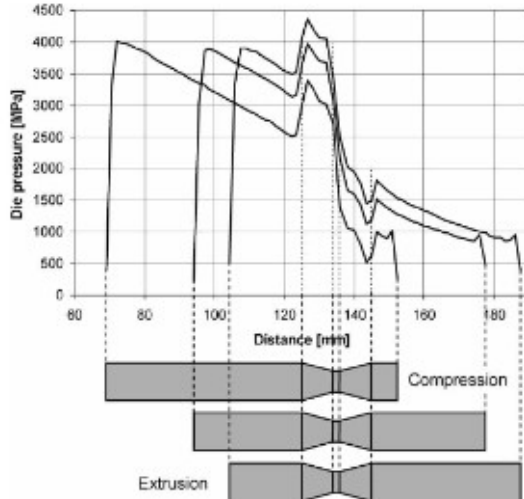


**Figure 2.9** Snapshots of die pressure evolution during CEC

This is caused by the fact that any friction length decrement in the extrusion chamber is accompanied by an equal amount of friction length increment in the compression chamber. Figure 20 presents FEM simulation results for CEC in the form of three snapshots of die pressure distribution. These results have been obtained for a strain hardening, lowcarbon steel billet subjected to cold reduction from 15 to 11 mm (and compressed back to 15 mm) and for the capped Coulomb's friction law with a friction coefficient of 0.06; the counter-force was kept constant. As can be seen in Fig. 20, the maximum die pressure in the extrusion chamber does not decrease during the process while the pressure level in the compression chamber and the conical part of the die increase.

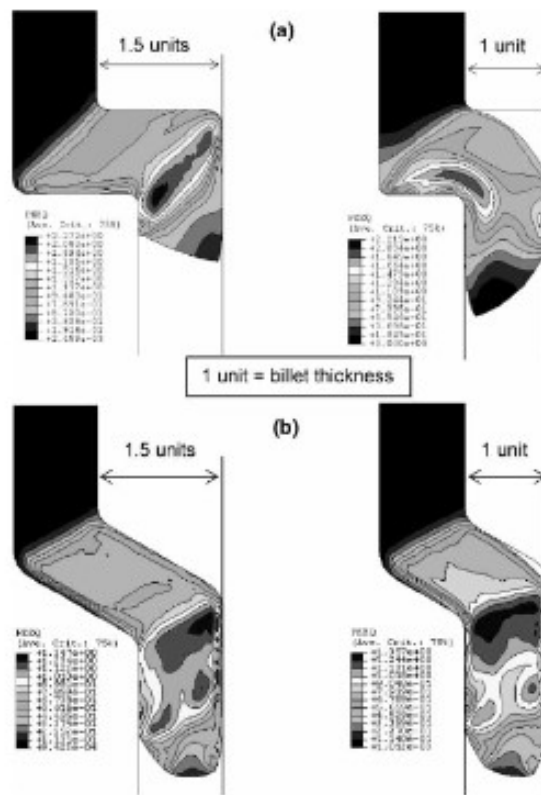


**Figure 130** Equivalent strain distribution for 1.5 and 1 unit offsets between the input and output passage in two-turn ECAP with 90°[7] (a) and 120°(b) angle between channel passages

The maximum die pressure approaches 4500 MPa, which is a high value even for superior tool materials. Reduction in the maximum tool pressure may be obtained by reducing the billet length or decreasing the material yield stress by carrying out the process at an elevated temperature. The counter-force has to remain above the compression yield level, which limits the possibility of its change. It might also be difficult to decrease friction coefficient below 0.06.

### 2.1.3 ECAP

In its basic form, ECAP is used with two channel passages (one channel turn) inclined at 90° (Fig. 22). The billet has to be subjected to several ECAP passes to accumulate a required strain. The billet is usually rotated about its axis by either 90° or 180° between the passes. In the attempt to reduce the number of passes, a two-turn, S-shape channel can be used [34–37, 45–48, 71]. The S-shape arrangement is equivalent to two passes in a one-turn ECAP with 180° billet rotation between the passes. Since this process is relatively new, an FEM simulation was carried out to help establish the appropriate channel geometry. It revealed that, for the 90° angle between channel passages, the offset between the input and the output passage should not be less than 1.5 channel thickness [36]. For the 120° angle the offset can be reduced to 1 channel thickness (Fig. 21). Reducing the passage offset by increasing the angle between passages helps minimize die dimensions, however, the amount of strain generated in one pass will decrease. On the other hand, the process force and tool stresses can be reduced. The above FEM simulation was carried out for square cross-section billets, which justified the use of the plane strain model. For round billets, a three dimensional simulation should be used to reveal details of non-uniform strain distribution during the process (Fig. 22(a)) [8]. In another new version of ECAP, known as three dimensional ECAP, a three turn channel is configured in the three orthogonal dimensions, which is equivalent to having two 90° billet rotations [72]. In this case, even for a square cross section, a three dimensional FEM simulation has to be used (Fig. 22(b)).

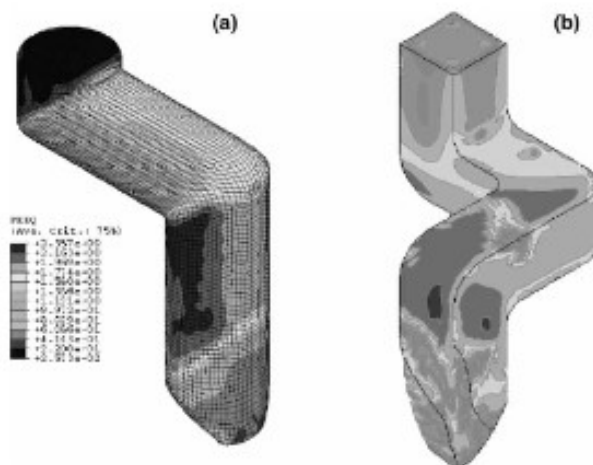


**Figure 2.11** Equivalent strain distribution in two-turn ECAP of a round billet [8] (a) and three-turn ECAP of a square billet (b) established by three-dimensional FEM analyses

### 2.1.3.1 Incremental ECAP

The I-ECAP process was invented as a result of FEM simulation experiments with shear deformation. The initial concept of repetitive shear (comparable with interrupted blanking operation without material fracture) has evolved into an ECAP-like incremental process, which can be applied to continuous billets. The last picture in Fig. 23 illustrates the process idea; a double-ended solid arrow indicates a reciprocating die whereas a dashed arrow represents the incremental feeding of the billet. Feeding takes place when there is no contact between the billet and the reciprocating die. This substantially reduces the feeding force. Shear deformation occurs in the dashed zone as a result of the reciprocating die coming into contact with the fixed billet. Thus, feeding and deformation have been separated. The process enables the use of much longer billets and, provided an appropriate feeding mechanism is used, also infinite billets. As a result, the main problem of short billets and poor utilization of the material that characterize many SPD processes has been overcome.

FEM analysis has been instrumental in designing the early versions of I-ECAP. For example, Fig. 24(a) shows that, for a 90° angle between channel passages, the angle at which a flat reciprocating die approaches the billet (the angle between the reciprocating movement and the feeding direction) should not be 0° because of a very high strain concentration and material folding (folding is not visible at the scale used in Fig. 24(a)). The same figure provides information on the billet bending caused by the reciprocating die, which is too short with respect to the stationary die, thus, not providing a symmetrical support for the processed billet. A possible remedy may lie in increasing the angle between channel passages to 110° and extending the reciprocating die to achieve a symmetrical billet support (Fig. 24(b)). Strain distribution is more uniform in this case, however, the attainable maximum strain is reduced. Another solution is to keep the 90° angle between channel passages and change the shape of the die by adding a spike which directs material flow into the output passage (Fig. 24(c)).

Finally, it is possible to retain the 90° angle between channel passages and use a flat reciprocating die while changing the direction of the reciprocating movement from 0° to, for example, 35° (Fig. 20(d)). This last case results in strain distribution which is very similar to one obtained in the classical ECAP provided that the feeding increment is not excessive compared with the billet thickness. In the simulations presented here, this increment was 10 percent of the billet thickness.

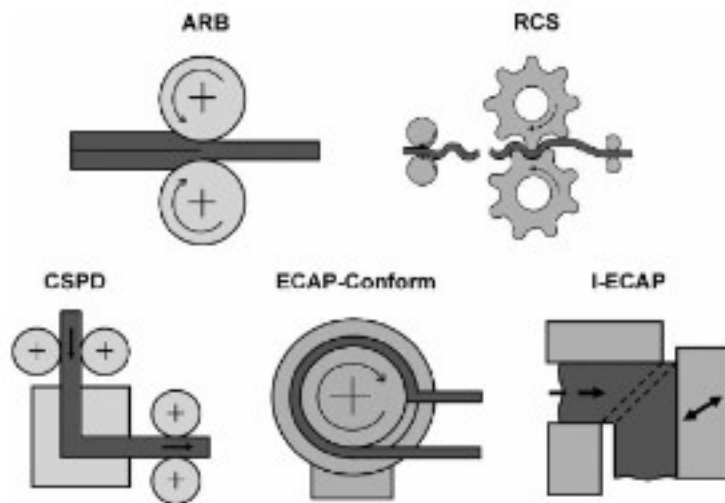
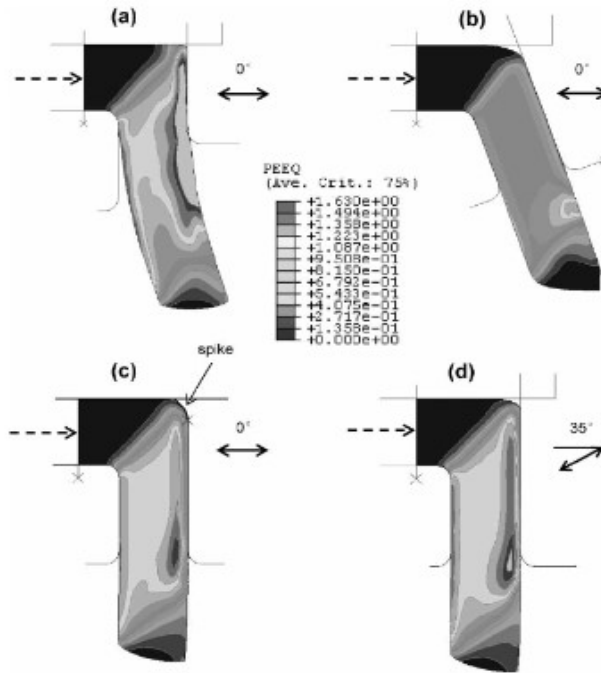


Figure 2.12 Continuous SPD processes



**Figure 2.13** Distribution of equivalent strain for different angle between channel passages, different size and shape of the reciprocating die and different direction of the reciprocating movement: (a) 90°, short flat die, 0°; (b) 110°, long flat die, 0°; (c) 90°, l

## 2.2 Case Setup

Information about the strain values of 27 different deformed parts will be explained step by step. As it mentioned before there are three main steps in the proposed methodology. These steps are decide on parts, drawing parts (in SolidWorks), Strain analysis of parts (in Deform). These steps are explained in a detailed manner below:

### 2.2.1 Determination of Parts

In this step, the parts that we will use in the analysis are decided. We decided to use 3 different pieces. these were the 30 degree, 45 degree and 60 degree parts respectively. Apart from that, Strain value is affected by Angle value as well as Pressing Speed and Friction Coefficient values. That's why we evaluated Angle, Pressing Speed and Friction Coefficient. and thus we obtained parts that reached 27 different Strain values.

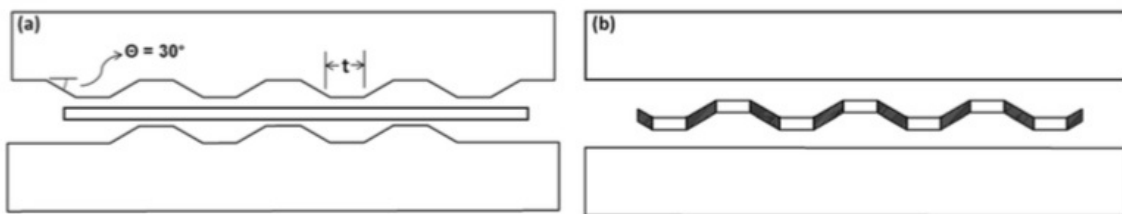


**Figure 2.14** Sample Piece

<b>Analysis No</b>	<b>Angle</b>	<b>Pressing Speed</b>	<b>Friction Coeficcident</b>
1	30	1	0,1
2	30	1	0,2
3	30	1	0,3
4	30	2	0,1
5	30	2	0,2
6	30	2	0,3
7	30	3	0,1
8	30	3	0,2
9	30	3	0,3
10	45	1	0,1
11	45	1	0,2
12	45	1	0,3
13	45	2	0,1
14	45	2	0,2
15	45	2	0,3
16	45	3	0,1
17	45	3	0,2
18	45	3	0,3
19	60	1	0,1
20	60	1	0,2
21	60	1	0,3
22	60	2	0,1
23	60	2	0,2
24	60	2	0,3
25	60	3	0,1
26	60	3	0,2
27	60	3	0,3

### 2.2.2 Drawing of Parts

The parts are designed according to the 30, 45 and 60 degree values given above.

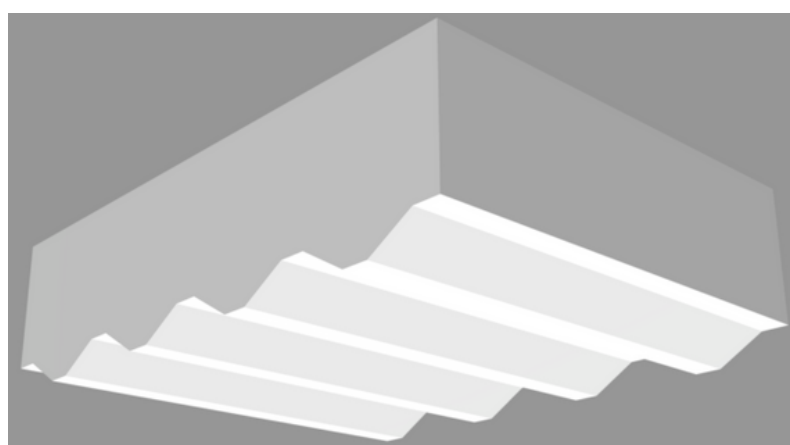


*Figure 2.I5 30° Top Die*

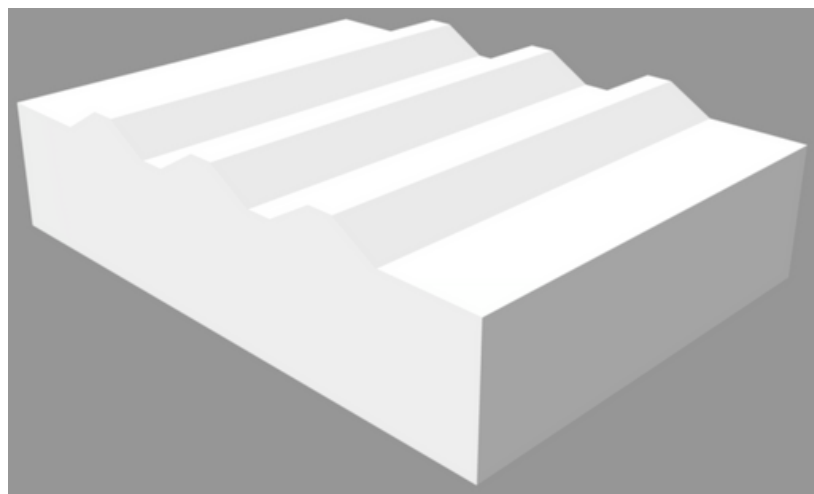


**Figure 2.16**  $30^\circ$  Bottom Die



**Figure 2.17**  $45^\circ$  Top Die



**Figure 2.18**  $45^\circ$  Bottom Die

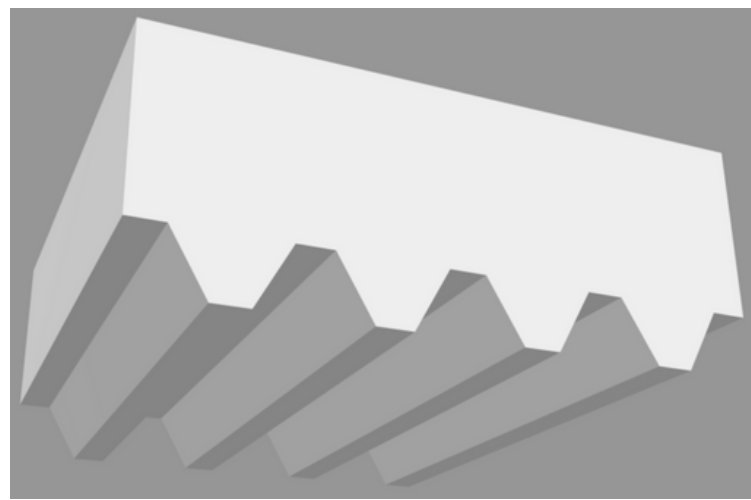


**Figure 2.19**  $60^\circ$  Top Die

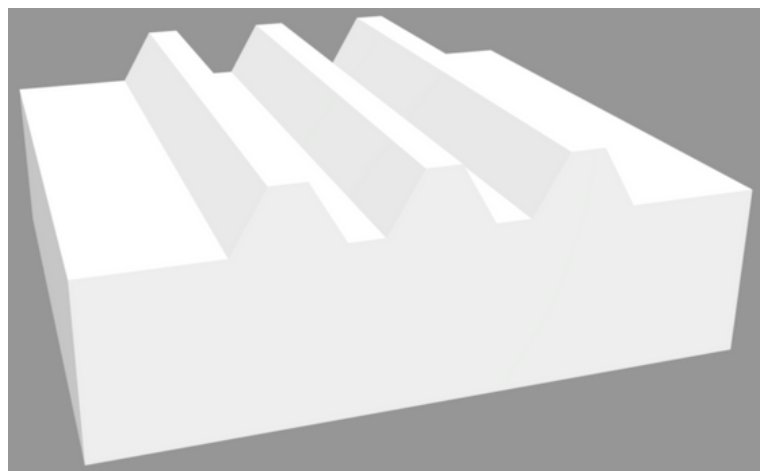


**Figure 2.20**  $60^\circ$  Bottom Die

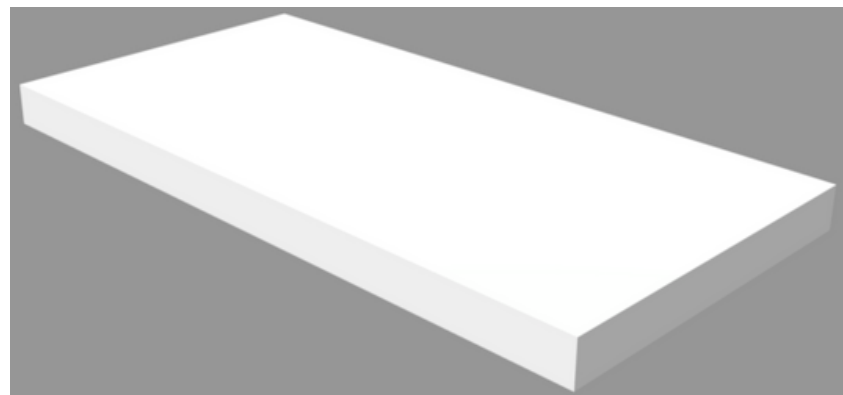


**Figure 2.21** Workpiece

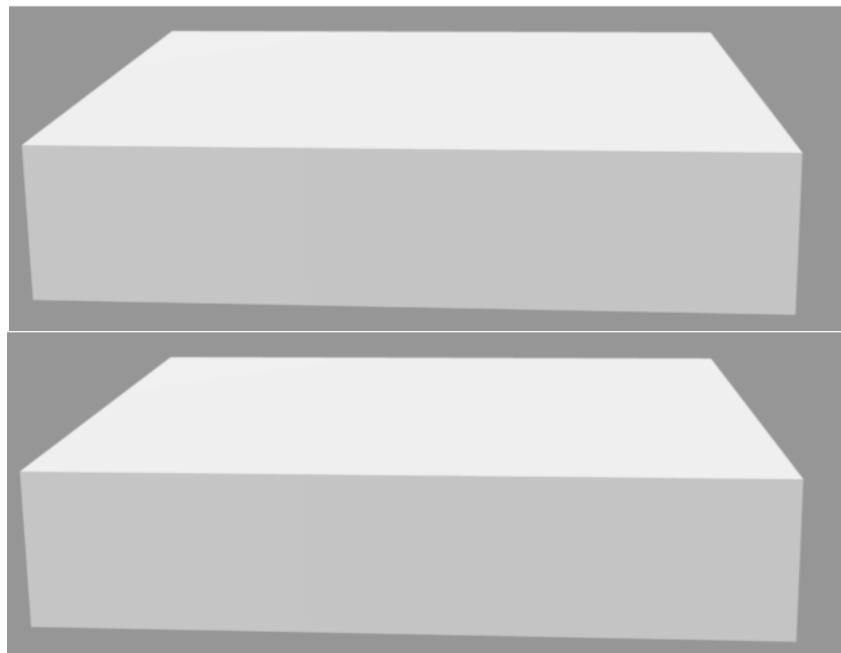


**Figure 2.22 Fix Pattern**

### 2.2.3 Strain Analysis of Parts

After designing the parts in SolidWorks, we transferred the parts to the Deform program. First we Meshed the Workpiece. After Meshing the Piece, we decided on the material of the Workpiece. The material was decided as AA6063 Aluminum. By doing these, we have adjusted the Workpiece.

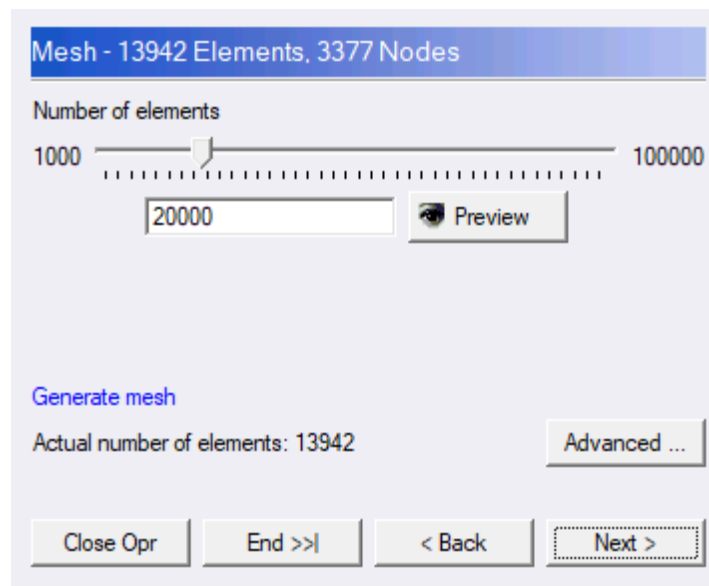


**Figure 2.23 Generate Mesh**

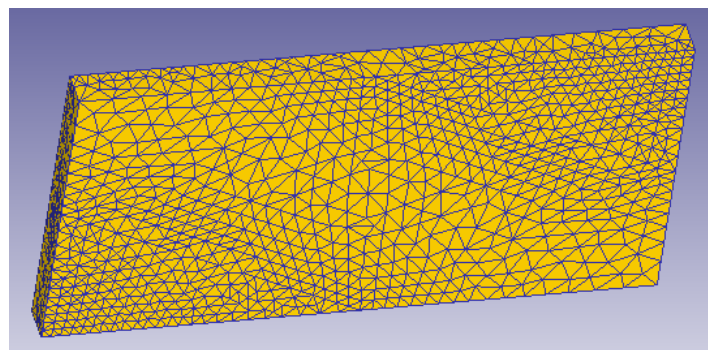


**Figure 2.24** Mesh Sheet

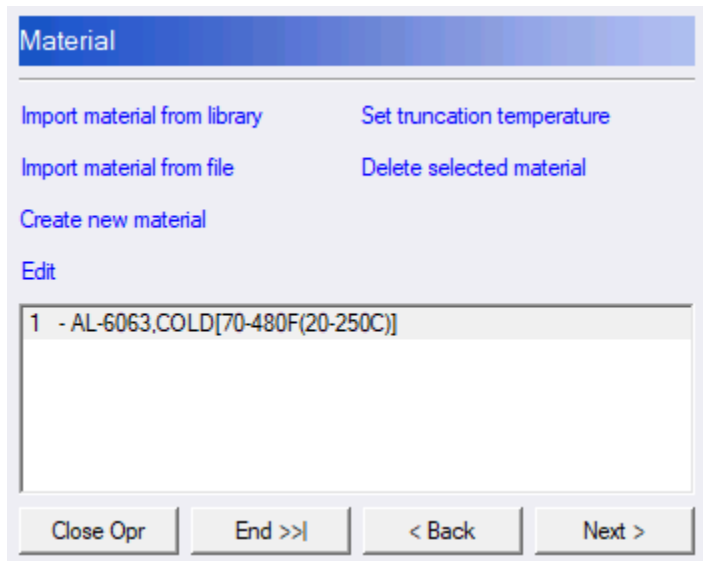


**Figure 2.25** Determination of Material

In the next step, we select the Top die part. After the part is selected, we determine the direction of movement for this part. and then we determine the speed of pressing this part.

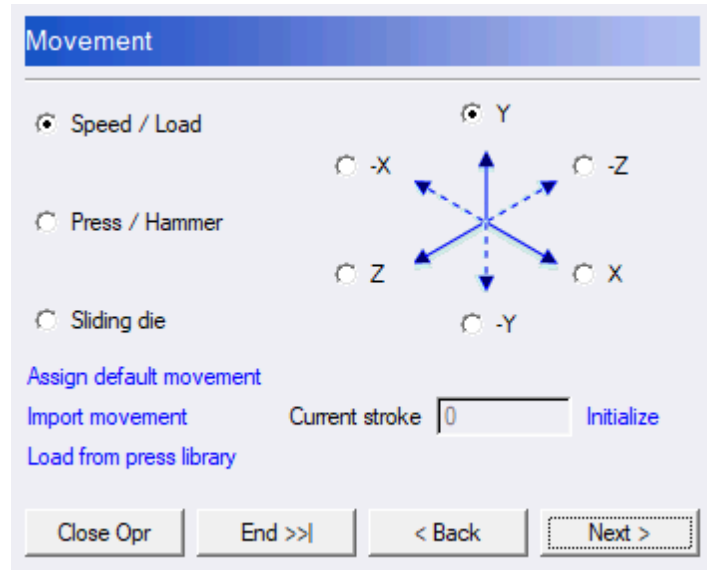


*Figure 2.26 Determination of Movement*

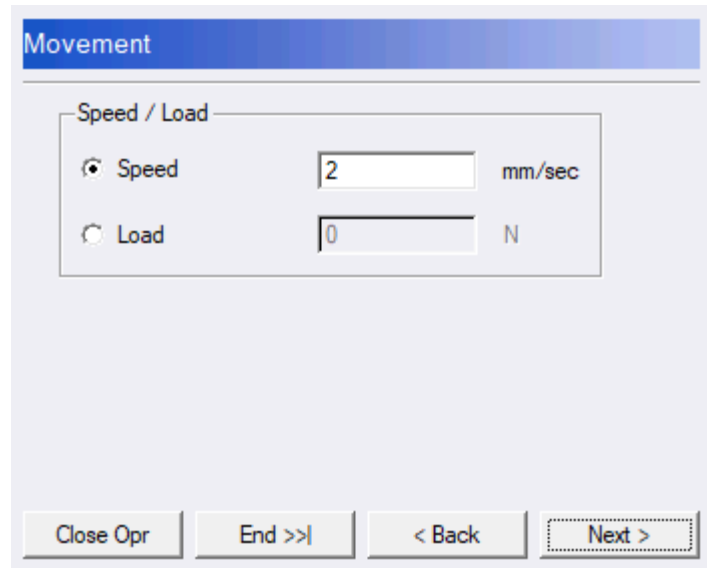


*Figure 2.27 Determination of Speed*

In the next step, bottom die is selected. After this piece is selected, the Friction Coefficient value is determined. and finally, these 3 parts are assembled in such a way that they come into contact with each other. As a result, we begin our Strain analysis. Each analysis consists of 4 steps. The first step is the pressing step. In this step, pressure is applied to the part. In the second step, the Workpiece is taken between 2 flat pieces, straightened and restored. In the third step, pressing the Workpiece is applied again. In the fourth step, the workpiece is again placed between two flat pieces, flattened and restored. these steps are applied to complete the analysis of each piece. An analysis is completed at the end of every four steps. Thus, we have performed a total of 27 analyzes.

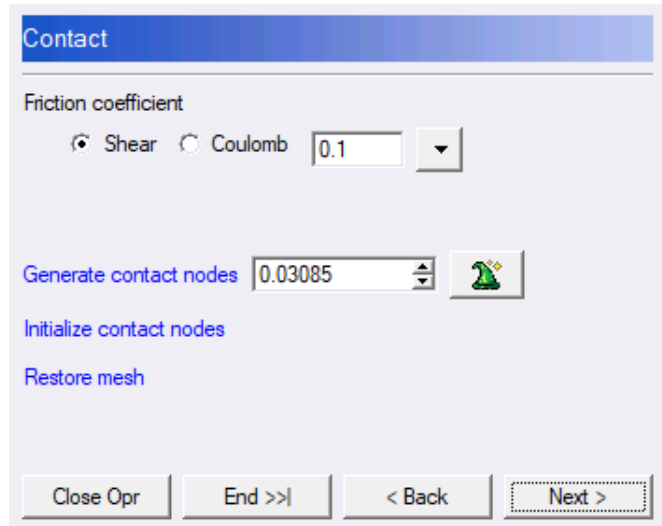


Figure 2.28 Determination of Friction Coefficient

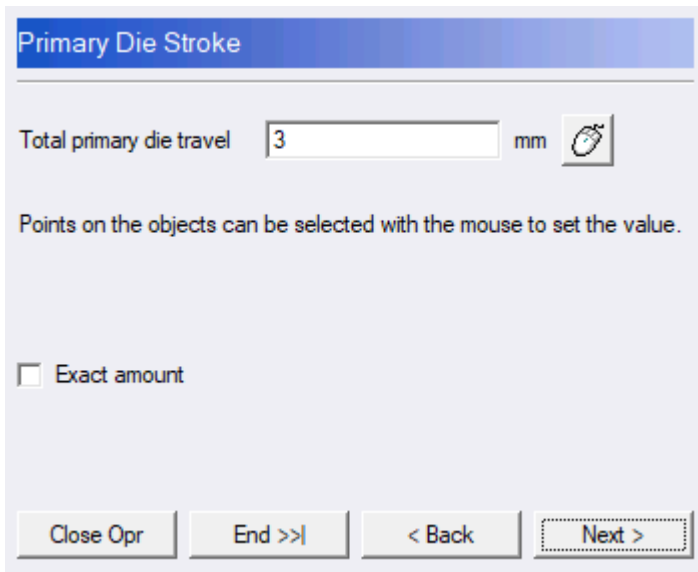
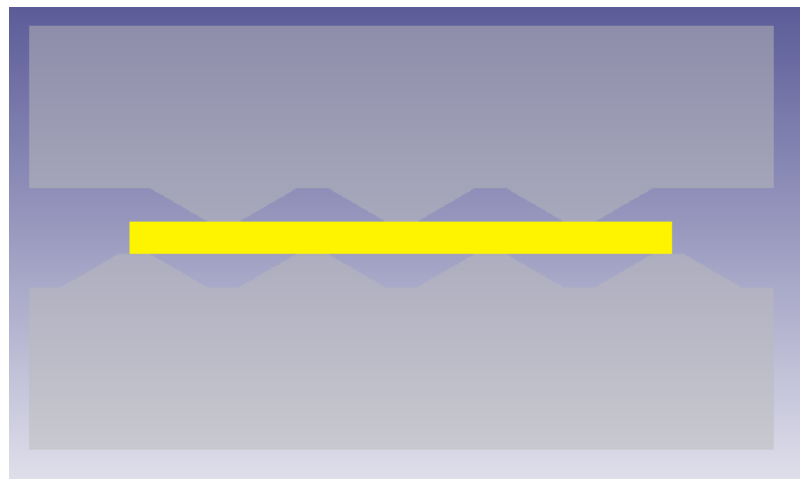
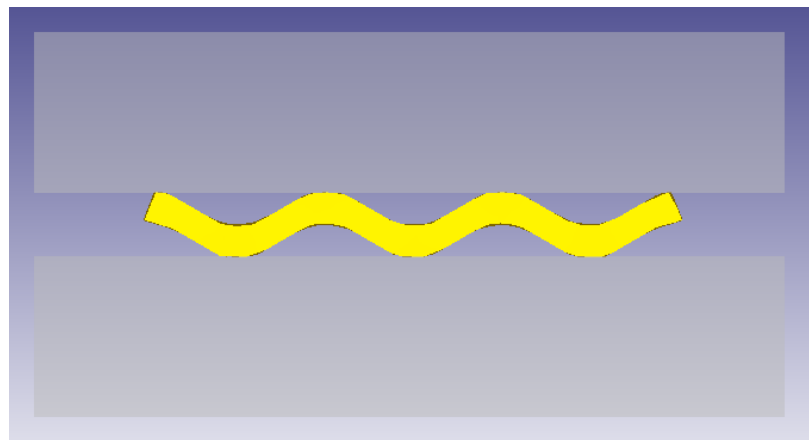


Figure 2.29 Determination of Stroke



**Figure 2.30** First Step



**Figure 2.31** Second Step

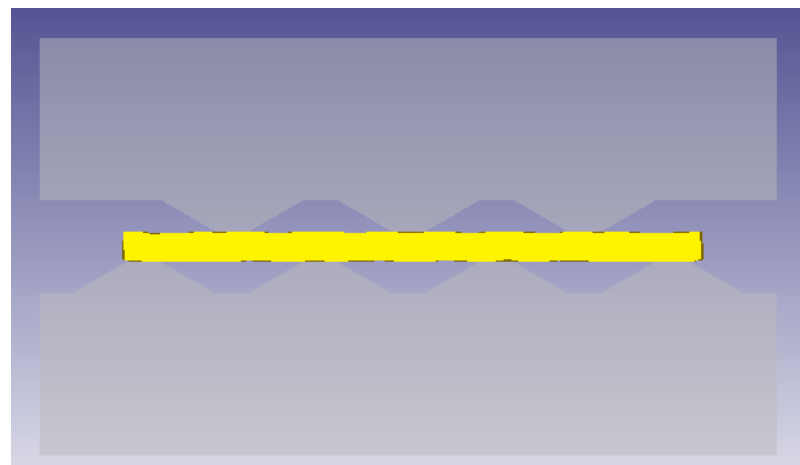


**Figure 2.32** Third Step

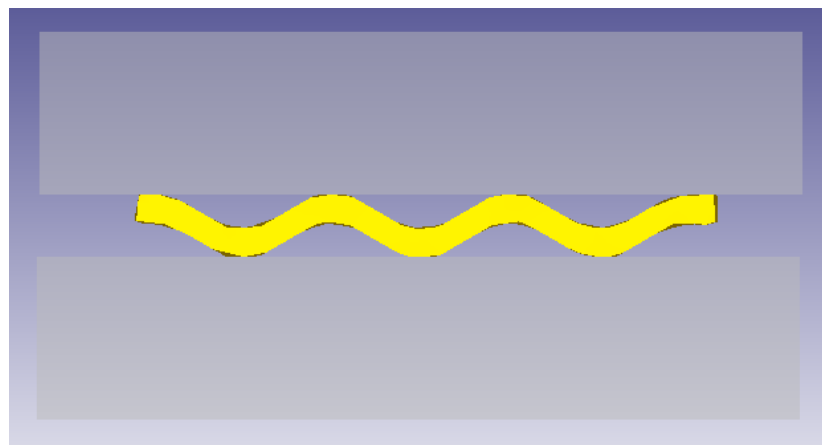


*Figure 2.33 Forth Step*

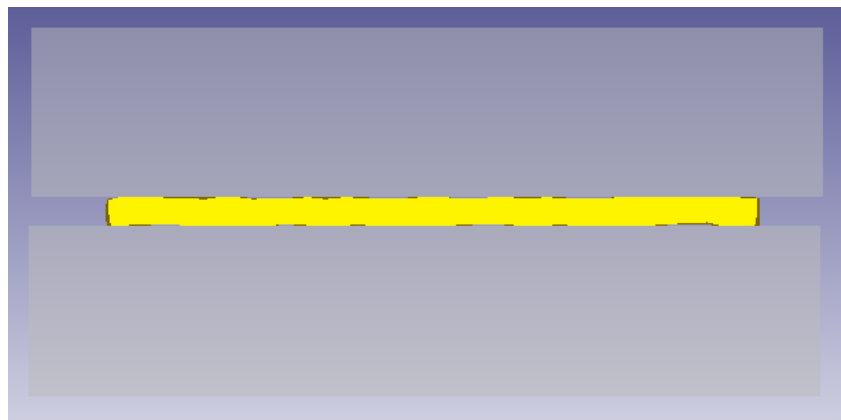


*Figure 2.34 Final Step*

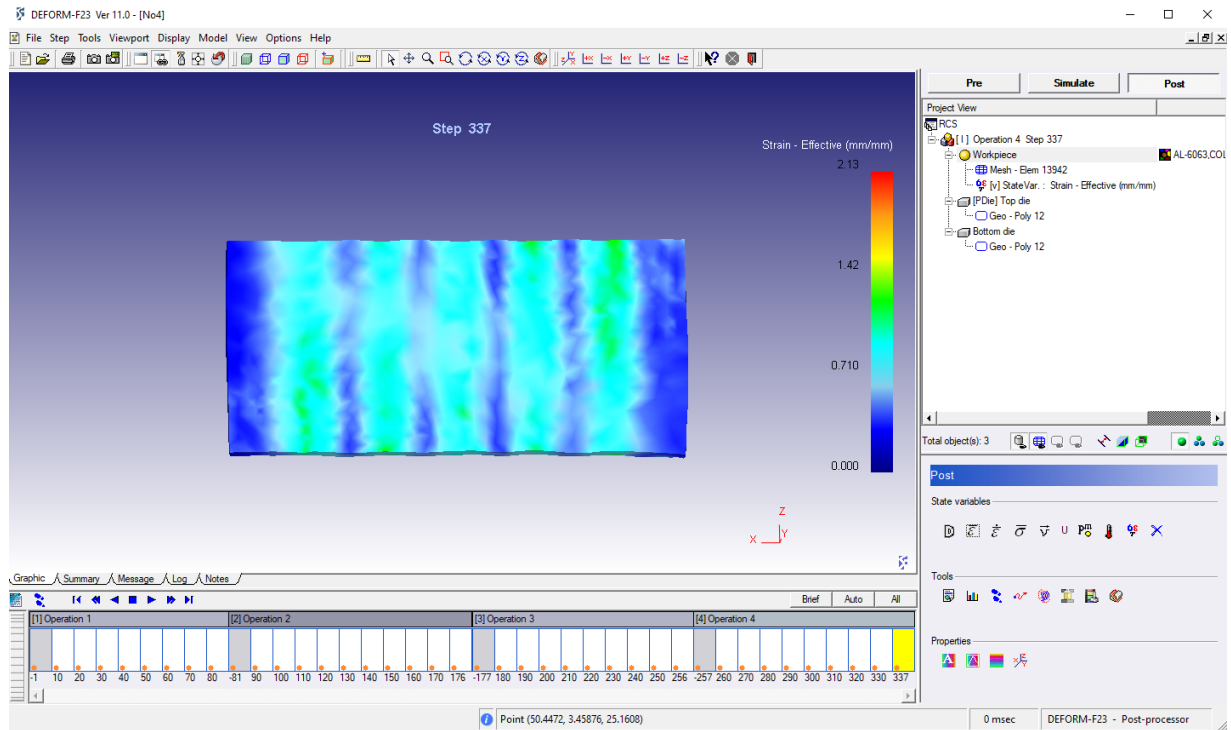


Figure 2.35 Strain Regions of the Deformed Part

In order to determine the strain value for each analysis performed, we determined 50 data points from each part. Then a strain graph was created by taking Strain values from these points.

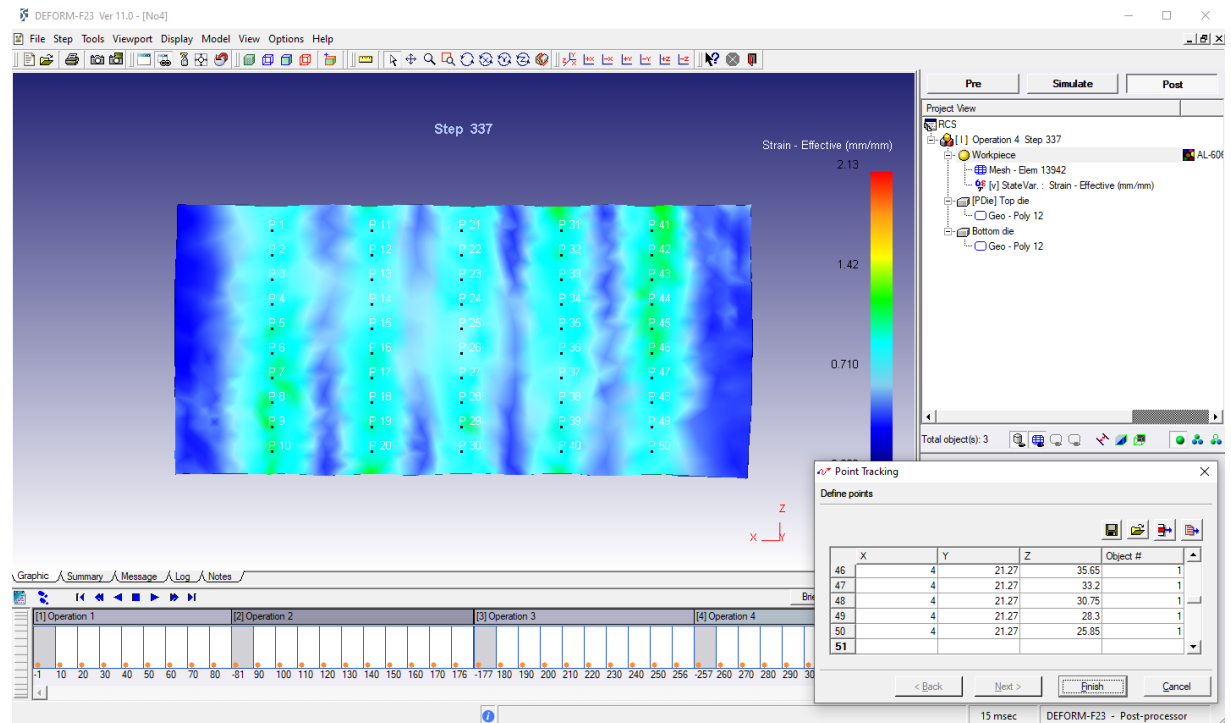
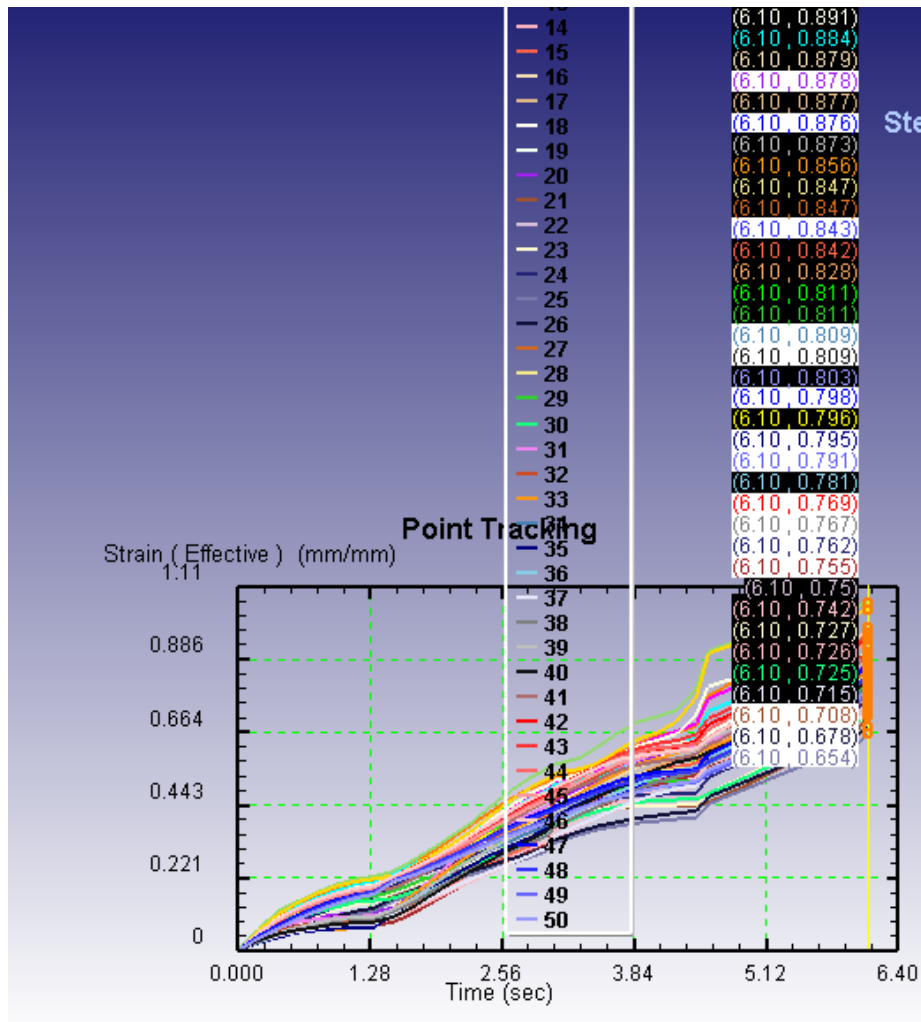


Figure 2.36 50 Points of Strain Regions



**Figure 2.37** Strain Values of Each Point Can Be Obtained

As the next step, we collected the Strain data that we obtained as a result of each of the 27 analyzes. and we calculated the arithmetic mean and standard deviation of these data. Then we calculated the strain inhomogeneity values by making the standard deviation divided by the arithmetic mean.

$$\frac{\text{Standard Deviation}}{\text{Arithmetic Mean}}$$

**Figure 2.38** Strain Inhomogeneity Equation

**Table 2.1 Results of Strain Inhomogeneity**

Analysis No	Angle	Pressing Speed	Friction Coefficient	Standard Deviation	Arithmetic Mean	Strain Inhomogeneity
1	30	1	0,1	0,096281969	0,756365698	0,127295526
2	30	1	0,2	0,070536825	0,420745976	0,167647059
3	30	1	0,3	0,094366951	0,769426397	0,122645845
4	30	2	0,1	0,091158815	0,840679525	0,108434679
5	30	2	0,2	0,102060788	0,760481307	0,134205519
6	30	2	0,3	0,104798141	0,768100801	0,136438005
7	30	3	0,1	0,081329013	0,76795736	0,105903032
8	30	3	0,2	0,095250184	0,756210996	0,125957152
9	30	3	0,3	0,103214849	0,763722676	0,135147027
10	45	1	0,1	0,140946637	1,117594788	0,126116047
11	45	1	0,2	0,098161286	1,195814528	0,082087384
12	45	1	0,3	0,096393239	1,218358051	0,079117332
13	45	2	0,1	0,092126553	1,168953579	0,078811131
14	45	2	0,2	0,118395839	1,184935195	0,099917565
15	45	2	0,3	0,109547486	1,154147903	0,094916333
16	45	3	0,1	0,098119069	1,144153297	0,085756926
17	45	3	0,2	0,109451227	1,120651875	0,097667464
18	45	3	0,3	0,129396985	1,098426073	0,117802179
19	60	1	0,1	0,210443007	1,748178353	0,120378454
20	60	1	0,2	0,132001748	1,815364623	0,072713628
21	60	1	0,3	0,220131045	1,789421297	0,123018009
22	60	2	0,1	0,192740469	1,78226002	0,108143855
23	60	2	0,2	0,17118596	1,919451701	0,089184823
24	60	2	0,3	0,161078504	1,769515594	0,091029717
25	60	3	0,1	0,102217487	1,762783162	0,057986421
26	60	3	0,2	0,191983726	1,875898087	0,102342301
27	60	3	0,3	0,176287249	1,814287712	0,097166093

Three graphs were created according to the velocity value of 1, 2 and 3 mm/sec.

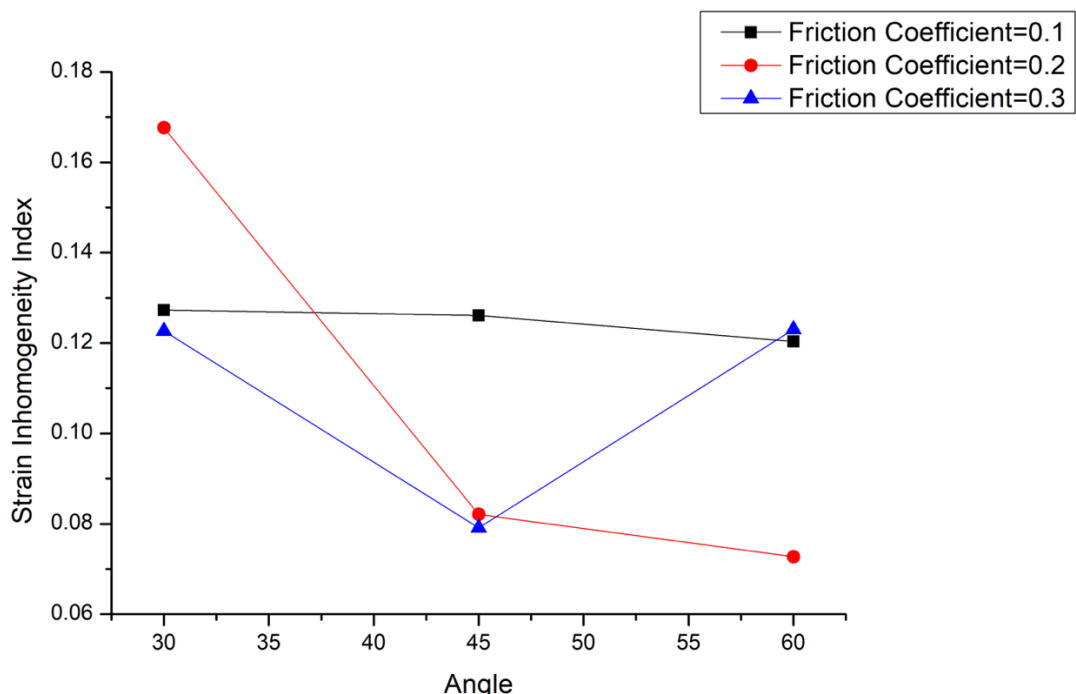


**Figure 2.39 Strain Inhomogeneity Index Graph for Pressing Speed of 1 mm/s**

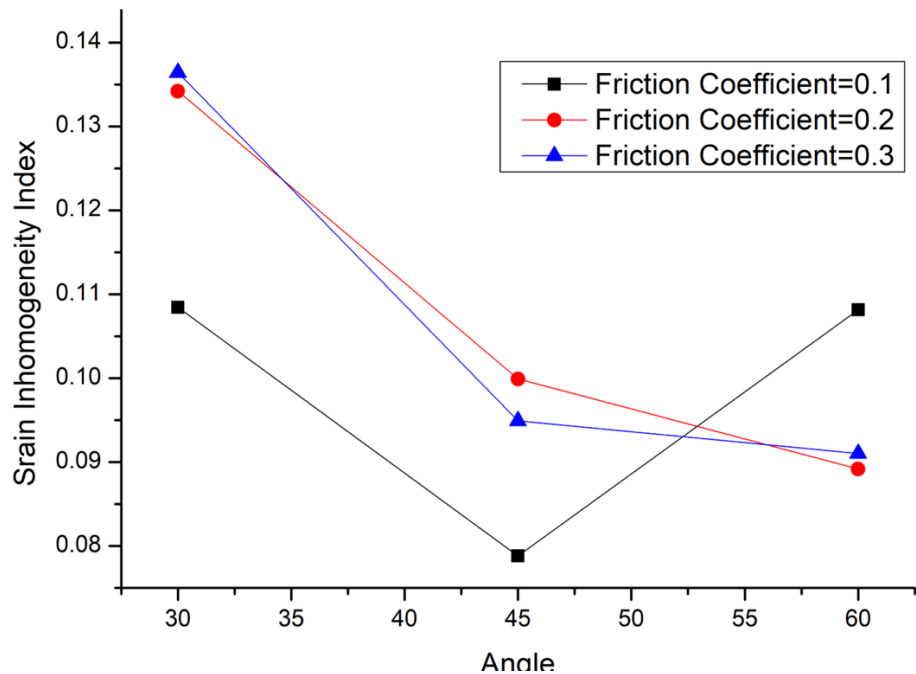


**Figure 2.40** Strain Inhomogeneity Index Graph for Pressing Speed of 2 mm/s

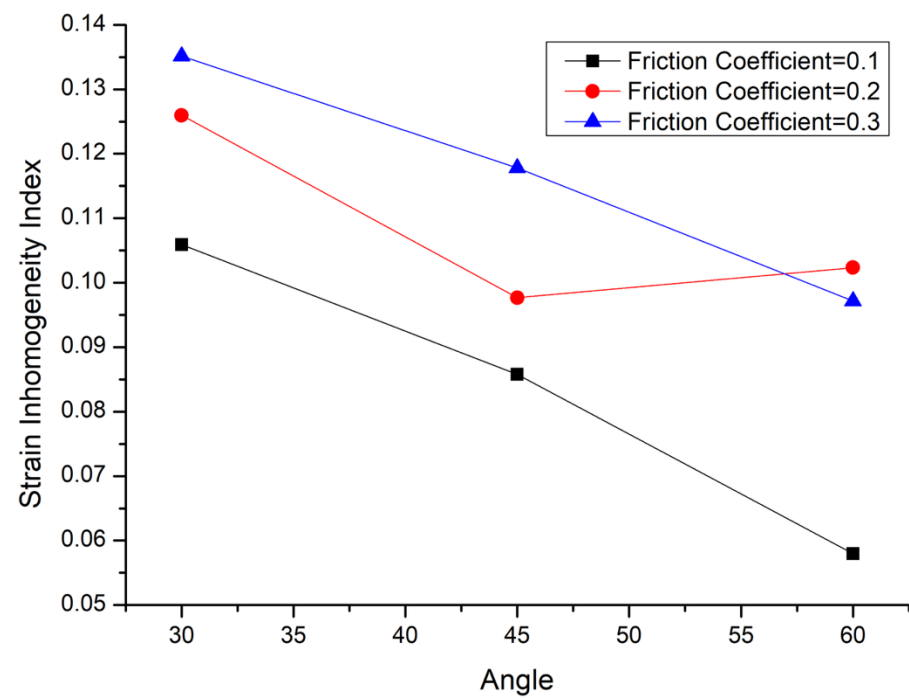


**Figure 2.41** Strain Inhomogeneity Index Graph for Pressing Speed of 3 mm/s

### 3. RESULTS AND DISCUSSION

Repetitive corrugation and straightening (RCS) is a process that induces cyclic plastic deformation on sheet geometries, reporting promising improvements in mechanical properties in metals and alloys. Alternative die geometries, as well as the effect of the process over strainhardenable alloys, have not been widely studied. In this work, sheets of the aluminum 5754 alloy were processed by RCS, using a novel die design to induce heterogeneous repetitive plastic deformation at room temperature. Numerical 3D Finite Element Analysis (FEA) was performed using the new die; the changes in the homogeneity of deformation, ductility and mechanical strength due to the process were studied. The processed samples were mechanically characterized by means of microhardness and tensile tests. Global and local XRD peak broadening were measured for determining the microstrain evolution during the process. After the initial heterogeneous RCS pass, a decrement in ductility was observed, but the increase in yield strength was significant. The microhardness mapping showed a heterogeneous distribution of the deformation with good agreement with the numerical simulation. XRD peaks width enlarged with the heterogeneous RCS passes in concordance with the mechanical results.[64]

The numerical simulations, shown in Fig. 25b and d, support the deformation distribution since they display a rather similar distribution of microhardness. On the other hand, the amount of deformation calculated showed a maximum of 1.89 and a minimum of 0.16, after the first pass of heterogeneous RCS. In the upper and the lower faces (Fig. 26), some differences in the deformation were also observed. The transition between the highly and less deformed zones is less abrupt in the upper face. In the second pass, the values of the deformation increased to a maximum of 2.37 and a minimum of 0.38. No difference between the upper and the lower faces, due to the 180° flip carried out before the second pass, was observed. It appears, from the numerical simulations, that the repetition of passes increased the level of plastic deformation within the sample, which ultimately increased the yield strength. It is important to note that the RCS process was only investigated for two passes, considering a no damage standard model of plasticity, as no cracks were experimentally observed. For a large number of passes, it would be necessary to assess the effect of damage on strengthening, using a model of plasticity that includes shear damage [74]. Comparison between the microhardness mapping and the corresponding FEA area showed good agreement between the hardness and equivalent plastic deformation distribution (Fig. 20). For the sample with one heterogeneous RCS pass, the zones with the highest microhardness (106 HV0.1) corresponded to a maximum strain of 1.89. Therefore, this FEA model could be used for predicting the deformation pattern and its corresponding qualitative microhardness mapping.

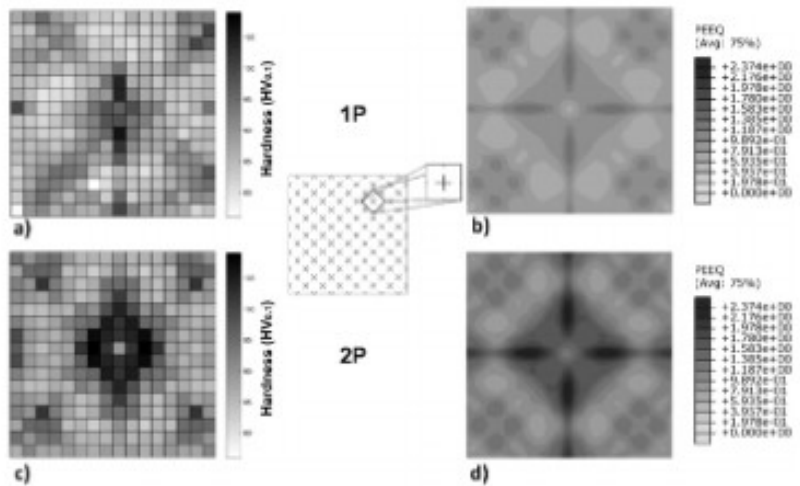


**Figure 3.1** Microhardness mapping for the samples processed by (a) 1 pass and (c) 2 passes of heterogeneous RCS and the numerical simulations for passes (b and d)

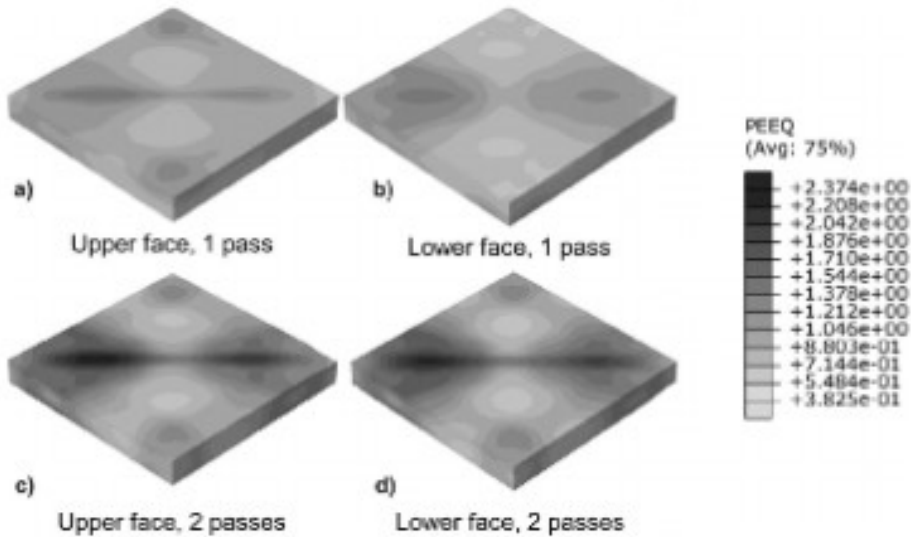


**Figure 3.2** Deformation distribution calculated for 1 pass of heterogeneous RCS in the (a) upper and (b) lower faces, (c and d) 2 passes sample of heterogeneous RCS for the upper and lower faces, respectively

Repetitive corrugation-straightening (RCS) and constrained groove pressing (CGP) are two promising severe plastic deformation techniques for sheet metallic materials. There are differences in amount of imposed plastic strain, hence, it is important to compare the deformation mode in these two techniques. In the present paper, the effect of RCS and CGP on the deformation behaviour of pure aluminium is studied. The effective parameters are analysed using finite element analysis (FEA) for one pass of deformation. The computer simulations are carried using DEFORM-3D and to verify the FEA results, a comparison with previous literatures is made. It is observed that filling ratio of the die is higher for CGP. Additionally, the deformed work-piece endured more plastic strain in CGP and the effective strain is more homogenously distributed in this technique. [75]

The commercial finite element method (FEM) software, Deform 3D<sup>TM</sup>, was used to perform the FEA of the deformation in RCS and CGP. The dies were modelled as rigid bodies. The work-piece was considered as samples with square cross section and dimensions of  $10 \times 10 \times 1$  mm<sup>3</sup> with 30,000 elements. The die design parameters as presented in Figures 1 and 2 are listed in Table 1. Pure aluminium was selected as a sheet material and its characteristics that were implemented in the simulation are defined with the help of software manual (Scientific Forming Technologies Corporation, 2006) and illustrated in Figure 3. The friction conditions between the surfaces of the sample and dies were considered as shear type with the coefficient of 0.1. All computer simulations were performed at a punch speed of 0.1 mm.s<sup>-1</sup> in isothermal conditions at room temperature.

**Table 3.1** Die design parameters used in the present study

SPD technique	Die design parameters	
	$\theta$ (°)	$t$ (mm)
CGP	45	1
RCS	45	1

In order to investigate the effect of RCS and CGP on the homogeneity of strain and deformation, The inhomogeneity index ( $C_i$ ) is used and presented in equation (1) [72] (Li et al., 2004):

*Eq. 2*

$$C_i = \frac{\varepsilon_{\max} - \varepsilon_{\min}}{\varepsilon_{avg}}$$

where  $\varepsilon_{\max}$ ,  $\varepsilon_{\min}$  and  $\varepsilon_{avg}$  are maximum, minimum and average effective strains, respectively. The effective strain distribution is considered homogenous at low value of  $C_i$ .

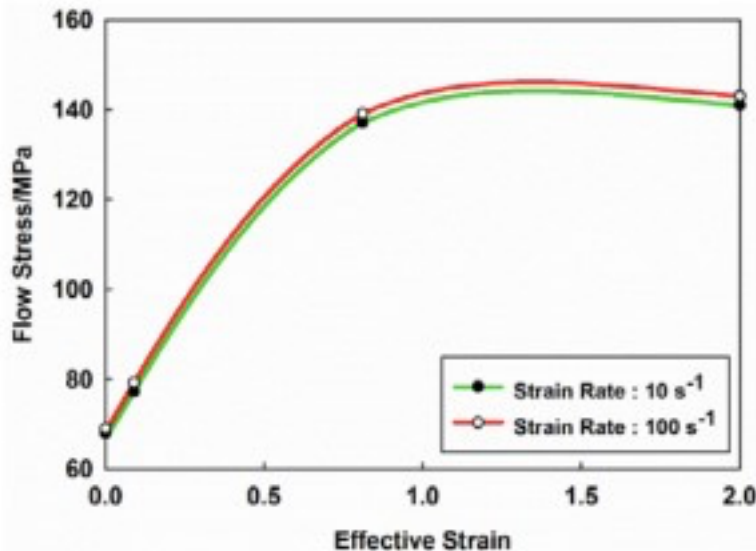


*Figure 3.3* Flow stress of pure aluminium implemented in FEA (see online version for colours)

To verify the accuracy of the computer simulations, FEA results of CGP process are compared with the results of Ghazani and Vajd (2014). Figure 27 shows a comparison between inhomogeneity indices of the effective strain distributions achieved from FEA results and Ghazani after one pass of CGP processing. One may see that this figure shows a good agreement between the FEA and results of Ghazani. In that way, the conditions, i.e., coefficient of friction and upper die speed, that were implemented in the simulation for CGP is as similar as those are reported (Ghazani and Vajd, 2014). [76]

Three graphs were created according to the velocity value of 1, 2 and 3 mm/sec. And from these graphs we can get the following information: When the graphs are examined, it is seen that the friction coefficient and pressing speed do not have an obvious effect. When the effect of angle values is examined, it is seen that the Strain Inhomogeneity value generally tends to decrease with increasing angle. However, in some cases, it has been observed that the angle increase has the opposite effect. The most important reason for this is that Strain values are very sensitive to location selection.

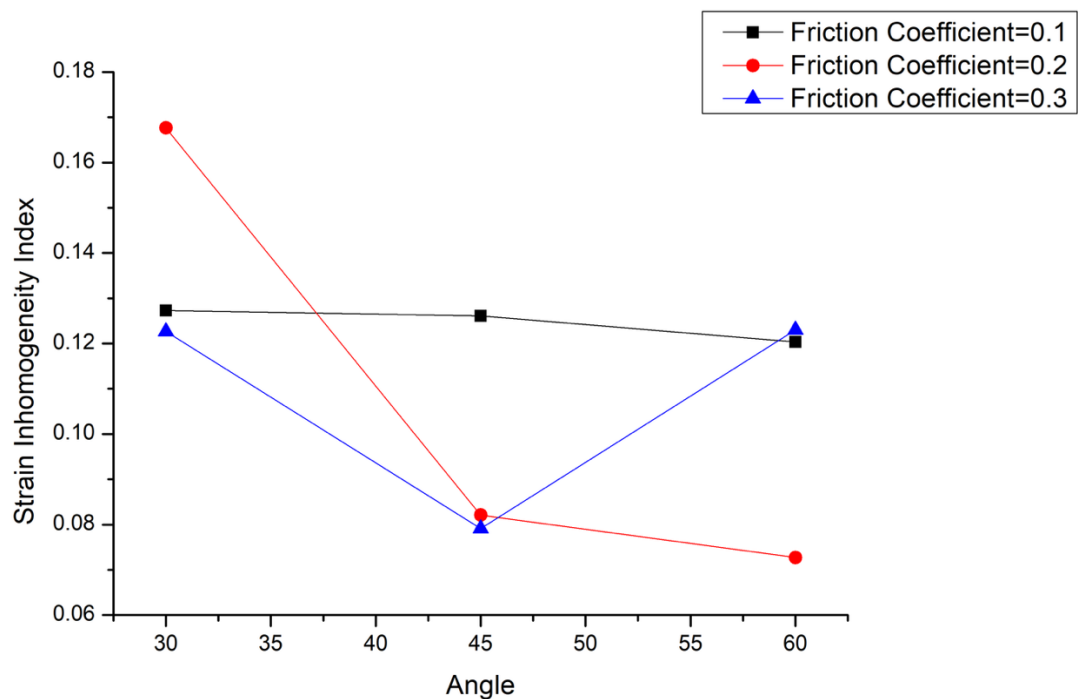


**Figure 3.4** Strain Inhomogeneity Index Graph for Pressing Speed of 1 mm/s

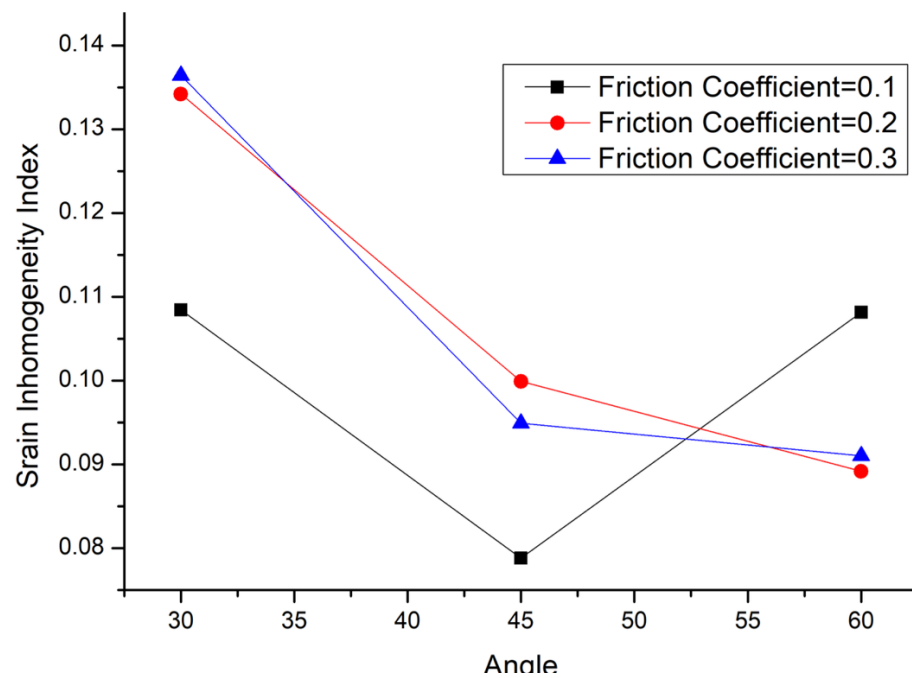


**Figure 3.5** Strain Inhomogeneity Index Graph for Pressing Speed of 2 mm/s

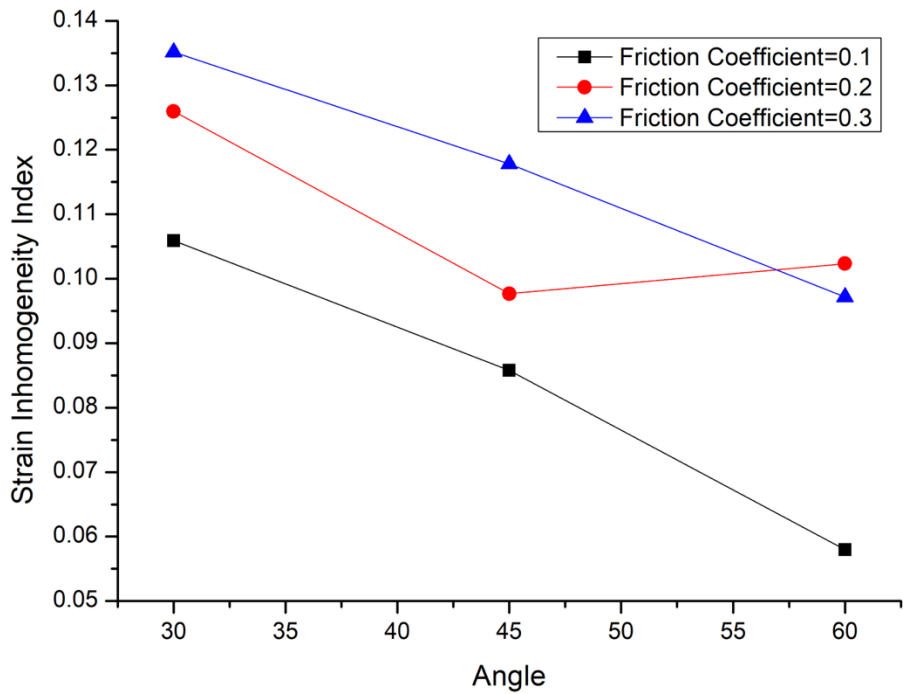


**Figure 3.6** Strain Inhomogeneity Index Graph for Pressing Speed of 3 mm/s

#### **4. CONCLUSION**

Within this study the effects of RCS channel angle, friction coefficient and pressing speed on strain inhomogeneity were investigated. For this purpose 27 finite elements analyses were performed. After that, strain inhomogeneity values were calculated for each analysis. The results obtained are as follow: There is no significant effects of pressing speed and friction coefficient on strain inhomogeneity. It is concluded that the strain inhomogeneity decreases with increasing angle. However, there are some exceptions for this statement since the applied method is sensitive to point selection.

The parts that we will use in the analysis are decided. We decided to use 3 different pieces. these were the 30 degree, 45 degree and 60 degree parts respectively. Apart from that, Strain value is affected by Angle value as well as Pressing Speed and Friction Coefficient values. That's why we evaluated Angle, Pressing Speed and Friction Coefficient. and thus we obtained parts that reached 27 different Strain values. After designing the parts in SolidWorks, we transferred the parts to the Deform program. First we Meshed the Workpiece. After Meshing the Piece, we decided on the material of the Workpiece. The material was decided as AA6063 Aluminum. By doing these, we have adjusted the Workpiece. Selected the Top die part. After the part is selected, we determine the direction of movement for this part. and then we determine the speed of pressing this part. In the next step, bottom die is selected. After this piece is selected, the Friction Coefficient value is determined. and finally, these 3 parts are assembled in such a way that they come into contact with each other. As a result, we begin our Strain analysis. Each analysis consists of 4 steps. The first step is the pressing step. In this step, pressure is applied to the part. In the second step, the Workpiece is taken between 2 flat pieces, straightened and restored. In the third step, pressing the Workpiece is applied again. In the fourth step, the workpiece is again placed between two flat pieces, flattened and restored. these steps are applied to complete the analysis of each piece. An analysis is completed at the end of every four steps. Thus, we have performed a total of 27 analyzes.

Three graphs were created according to the velocity value of 1, 2 and 3 mm/sec. And from these graphs we can get the following information: When the graphs are examined, it is seen that the friction coefficient and pressing speed do not have an obvious effect. When the effect of angle values is examined, it is seen that the Strain Inhomogeneity value generally tends to decrease with increasing angle. However, in some cases, it has been observed that the angle increase has the opposite effect. The most important reason for this is that Strain values are very sensitive to location selection.

## 5. REFERENCES

- 1) Antti Korhonen, Severe plastic deformation (SPD) process for metals, 2008.09.005
- 2) Segal V 2018 Review: Modes and Processes of Severe Plastic Deformation (SPD) Materials (Basel).
- 3) Nanostructured Copper , Zhu Y T, Jiang H., 2000
- 4) Bulk Nanostructured Metals ,Yuntian T, Lowe,Terry C, 2001 5) Copper by J.Y. Huang,Y.T. Zhu,H. Jiang,T.C. Lowe. , 2001
- 6) Nanocrystalline ,by JY Huang, XZ Liao, YT Zhu , F Zhou, 2003
- 7) Copper ,Jianyu Huang,Yuntian T. Zhu,David J. Alexander,Xiaozhou Liao,Terry C. Lowe,Robert J. Asaro. , 2004
- 8) Al and Al–0.25Sc alloy ,V. Rajinikanth, Gaurav Arora, N. Narasaiah, K. Venkateswarlu. , 2008
- 9) Pure aluminium , A. Krishnaiah & H. S. Kim. , 2008
- 10) Pure Al , Dimitry Orlow. , 2008
- 11) CuCr0.6 alloy , J. Stobrawa, Z. Rdzawski , W. Głuchowski , W. Malec. , 2009
- 12) CuNi2Si1alloy , Zbigniew Rdzawski, W Gluchowski., 2009
- 13) CuCr0,6 , J.P. Stobrawa , Z.M. Rdzawski , W. Głuchowski , W. Malec. , 2009
- 14) Duratherm 600 cobalt superalloy , H. Sheikh. , 2010
- 15) Low carbon steel , by F. Khodabakhshi, M. Kazeminezhad, A.H. Kokabi. , 2010 16) Precipitation hardened copper alloys , J. Stobrawa, Z. Rdzawski. , 2011
- 17) Al–Cu and Al–Cu–Sc alloys , by S.C. Pandey, M.A. Joseph,M.S. Pradeep,K. Raghavendra,V.R. Ranganath,K. Venkateswarlu, Terence G. Langdon. , 2012
- 18) Al sheets , Susheelkumar Vijapur, M Krishna, H N Narasimha Murthy. , 2012
- 19) Martensitic steel , Arya Mirsepasi,Mahmoud Nili-Ahmabadabi,Mohammad HabibiParsa,Hadi Ghasemi-Nanesa,Ahmad F. Dizaji., 2012
- 20) Aluminum , H. S. Siddesha., 2012
- 21) CuSn6 alloy , W. Kwaśny , P. Nuckowski , Z. Rdzawski , W. Głuchowski. , 2013
- 22) Steel sheets , F. Khodabakhshi, M. Abbaszadeh, H. Eskandari, S.R. Mohebpour., 2013
- 23) Sheet metals, Sunil, B. Ratna, 16 October 2014
- 24) Aluminum Alloy(AA 5083),N. Thangapandian,S. Balasivanandha Prabu,23 July 2015
- 25) Austenitic Stainless Steel, Peyman Asghari Rad , Hassan Shirazi , Sebastian Koldorf , Mahmoud Nili-Ahmabadabi,12 November 2015
- 26) Al-3Mg and Al-3Mg-0.25Sc alloys, Prabhakar M Bhovi ,K. Venkateswarlu, 14 November 2015
- 27) Al–Mg alloy, N. Thangapandian,S. Balasivanandha Prabu,K.A. Padmanabhan, 1 January 2016
- 28) AA5083 Aluminum Alloy, N. Thangapandian, S.Balasivanandha Prabu & K. A. Padmanabhan, 19 January 2016
- 29) A356 Aluminum Alloy, Mahmoud Nili-Ahmabadabi , Hassan Shirazi, 12 May 2016
- 30) Al-Mg-Sc alloy, Prabhakar M. Bhovi,Deepak C. Patil,S.A. Kori,K. Venkateswarlu,Yi Huang,Terence G. Langdon, October–December 2016
- 31) Al-Mg-Si Aluminium Alloy, N. Thangapandian , S. Balasivanandha Prabu, December 2016
- 32) Prangnell, P. B., Harris, C., and Roberts, S. M.Finite element modelling of equal channel angularextrusion. Scr. Mater., 1997, 37, 983–989.
- 33) DeLo, D. P. and Semiatin, S. L. Finite-element modellingof nonisothermal equalchannel angular extrusion. Met-all. Mater. Trans. A, 1999, 30A, 1391–1402.
- 34) Ono, M., Mizufune, H., and Narita, M. Develop-ment of semicontinuous 4-stage ECAE method. InAdvanced technology of plasticity 2002 (Eds N. Kiuchi,H. Nishimura, and J.

- Yanagimoto), in Proceedings of the 7th International Conference on Technology of Plasticity, Yokohama, Japan, 27 October–1 November 2002, pp.1249–1254 (Japan Society for Technology of Plasticity)
- 35) Raab, G. I. Plastic flow at equal channel angular processing in parallel channels. *Mater. Sci. Eng.*, 2005, A410–411,230–233.
  - 36) Rosochowski, A. and Olejnik, L. Numerical and physical modelling of plastic deformation in 2-turn equal channel angular extrusion. *J. Mater. Process. Technol.*, 2002,125–126, 309–316.
  - 37) Rosochowski, A., Olejnik, L., and Balendra, R. FEM analysis of two-turn equal channel angular extrusion of cylindrical billets. In Esaform 2004 (Ed. S. Storen), in Proceedings of the 7th International Conference on Material Forming, Trondheim, Norway, 28–30 April 2004,pp. 207–210 (Norwegian University of Science and Technology).
  - 38) Li, S., Bourke, M. A. M., Beyerlein, I. J., Alexander, D. J., and Clausen, B. Finite element analysis of the plastic deformation zone and working load in equal channel angular extrusion. *Mater. Sci. Eng.*, 2004, A382,217–236.
  - 39) Luis-Perez, C. J., Luri-Irigoyen, R., and Gastón-Ochoa, D. Finite element modelling of an Al–Mn alloy by equal channel angular extrusion (ECAE). *J. Mater. Process. Technol.*, 2004, 153–154, 846–852.
  - 40) Nagasekhar, A. V. and Tick-Hon, Y. Optimal tool angles for equal channel angular extrusion of strain hardening materials by finite element analysis. *Comp. Mater. Sci.*,2004, 30, 489–495.
  - 41) Son, I. H., Lee, J. H., and Im, Y. T. Finite element investigation of equal channel angular extrusion with backpressure. *J. Mater. Process. Technol.*, 2006, 171, 480–487.
  - 42) Srinivasan, R. Computer simulation of the equichannel angular extrusion (ECAE) process. *Scr. Mater.*, 2001, 44,91–96.
  - 43) Alkorta, J. and Sevillano, J. G. A comparison of FEM and upper-bound type analysis of equal-channel angular pressing (ECAP). *J. Mater. Process. Technol.*, 2003, 141,313–318.
  - 44) Dumoulin, S., Roven, H. J., Werenskiold, J. C., and Valberg, H. S. Finite element modeling of equal channel angular pressing: effect of material properties, friction and die geometry. *Mater. Sci. Eng.*, 2005, A410–411,248–251.
  - 45) Yang, F., Saran, A., and Okazaki, K. Finite element simulation of equal channel angular extrusion. *J. Mater. Process. Technol.*, 2005, 166, 71–78.
  - 46) Králícs, G., Budilov, I. N., Alexandrov, I. V., Raab, G.I., Zhernakov, V. S., and Valiev, R. Z. Computer simulation of equal-channel angular pressing of tungsten by means of the finite element method. In NanoSPD2(Eds M. J. Zehetbauer and R. Z. Valiev), in Proceedings of the Conference on Nanomaterials by Severe Plastic Deformation, Vienna, Austria, 9–13 December 2002,pp. 271–277 (Wiley-VCH, Weinheim).
  - 47) Zuyan, L., Gang, L., and Wang, Z. R. Finite element simulation of a new deformation type occurring in changing channel extrusion. *J. Mater. Process. Technol.*, 2000, 102,30–32.
  - 48) Kim, H. S. Finite element analysis of deformation behaviour of metals during equal channel multi-angular pressing. *Mater. Sci. Eng.*, 2002, A328, 317–323.
  - 49) Bowen, J. R., Ghosh, A., Roberts, S. M., and Prangnell, P. B . Analysis of the billet deformation behaviour in equal channel angular extrusion. *Mater. Sci. Eng.*, 2000, A287,87–99.
  - 50) Oruganti, R. K., Subramanian, P. R., Marte, J. S., Gigliotti, M. F., and Amacherla, S. Effect of friction, backpressure and strain rate sensitivity on material flow during equal channel angular extrusion. *Mater. Sci. Eng.*,2005, A406, 102–109.

- 51) Semiatin, S. L., DeLo, D. P., and Shell, E. B. The effect of material properties and tooling design on deformation and fracture during equal channel angular extrusion. *Acta Mater.*, 2000, 48, 1841–1851.
- 52) Suo, T., Li, Y., Guo, Y., and Liu, Y. The simulation of deformation distribution during ECAP using 3D finite element method. *Mater. Sci. Eng.*, 2006, A432, 269–274.
- 53) Chung, S. W., Somekawa, H., Kinoshita, T., Kim, W. J., and Higashi, K. The nonuniform behavior during ECAE process by 3-D FVM simulation. *Scr. Mater.*, 2004, 50, 1079–1083.
- 54) Kim, W. J., Namgung, J. C., and Kim, J. K. Analysis of strain uniformity during multipressing in equal channel angular extrusion. *Scr. Mater.*, 2005, 53, 293–298.
- 55) Kim, H. S., Seo, M. H., and Hong, S. I. On the die corner gap formation in equal channel angular pressing. *Mater. Sci. Eng.*, 2000, A291, 86–90.
- 56) Li, S., Beyerlein, I. J., Necker, C. T., Alexander, D. J., and Bourke, M. Heterogeneity of deformation texture in equal channel angular extrusion of copper. *Acta Mater.*, 2004, 52, 4859–4875.
- 57) Figueiredo, R. B., Pinheiro, I. P., Aguilar, M. T. P., Modenesi, P. J., and Cetlin, P. R. The finite element analysis of equal channel angular pressing (ECAP) considering the strain path dependence of the work hardening of metals. *J. Mater. Process. Technol.*, 2006, 180, 30–36.
- 58) Figueiredo, R. B., Aguilar, M. T. P., and Cetlin, P. R. Finite element modelling of plastic instability during ECAP processing of flow-softening materials. *Mater. Sci. Eng.*, 2006, A430, 179–184.
- 59) Kim, S. H. Finite element analysis of equal channel angular pressing using a round corner die. *Mater. Sci. Eng.*, 2001, A315, 122–128.
- 60) Lee, S. C., Ha, S. Y., Kim, K. T., Hwang, S. M., Huh, L. M., and Chung, H. S. Finite element analysis for deformation behavior of an aluminum alloy composite containing SiC particles and porosities during ECAP. *Mater. Sci. Eng.*, 2004, A371, 306–312.
- 61) Baik, S. C., Estrin, Y., Kim, H. S., and Hellmig, R. J. Dislocation density-based modeling of deformation behavior of aluminium under equal channel angular pressing. *Mater. Sci. Eng.*, 2003, A351, 86–97.
- 62) Leo, P., Cerri, E., De Marco, P. P., and Roven, H. J. Properties and deformation behaviour of severe plastic deformed aluminium alloys. *J. Mater. Process. Technol.*, 2007, 182, 207–214.
- 63) Alexandrov, I. V., Budilov, I. N., Krallics, G., Kim, H. S., Yoon, S. C., Smolyakov, A. A., Korshunov, A. I., and Solovyev, V. P. Simulation of equal-channel angular pressing. In *NanoSPD3* (Ed. Z. Horita), in Proceedings of the 3rd International Conference on Nanomaterials by Severe Plastic Deformation, Fukuoka, Japan, 22–26 September 2005, *Mater. Sci. Forum*, 2006, 503–504, 201–208.
- 64) Rosochowski, A., Rodiet, R., and Lipinski, P. Finite element simulation of cyclic extrusion-compression. In *Metal forming 2000* (Eds M. Pietrzyk, J. Kusiak, and J. Majta), in Proceedings of the 8th International Conference on Metal Forming, Krakow, Poland, 3–7 September 2000, pp. 253–259 (A. A. Balkema, Rotterdam, Brookfield).
- 65) Kim, S. H. Finite element analysis of high pressure torsion processing. *J. Mater. Process. Technol.*, 2001, 113, 617–621.
- 66) Lee, J. W. and Park, J. J. Numerical and experimental investigations of constrained groove pressing and rolling for grain refinement. *J. Mater. Process. Technol.*, 2002, 130–131, 208–213.
- 67) Valiev, R. Z., Krasilnikov, N. A., and Tsenev, N. K. Plastic deformation of alloys with submicron-grained structure. *Mater. Sci. Eng.*, 1991, A137, 35–40.

- 68) Sakai, G., Nakamura, K., Horita, Z., and Langdon, T. G. Developing high-pressure torsion for use with bulk samples. *Mater. Sci. Eng.*, 2005, A406, 268–273.
- 69) Erbel, S. Mechanical properties and structure of extremely strainhardened copper. *Met. Technol.*, 1979, 12, 482–486.
- 70) Richert, J. and Richert, M. A new method for unlimited deformation of metals and alloys. *Aluminium*, 1986, 62, 604–607.
- 71) Nakashima, K., Horita, Z., Nemoto, M., and Langdon, T. G. Development of a multipass facility for equal-channel angular pressing to high total strains. *Mater. Sci. Eng.*, 2000, A281, 82–87.
- 72) Rosochowski, A., Olejnik, L., and Richert, M. 3D-ECAPOf square aluminium billets. In *Advanced methods in material forming* (Ed. D. Banabic) 2007, pp. 215–232 (Springer-Verlag, Berlin, Heidelberg, New York).
- 73) Marco Ezequiel, Ignacio A. Figueroa, Numerical and experimental study of a 5754aluminum alloy processed by heterogeneous repetitive corrugation and straightening, 2019.12.026
- 74) L Morin, JB Leblond, V Tvergaard Application of a model of plastic porous materials including void shape effects to the prediction of ductile failure under shear-dominated loadings *J Mech Phys Solids*, 94 (2016), pp. 148-166.
- 75) Farhad Rahimi; Bagher Mohammad Sadeghi; Masoud Ahmadi, Finite element analysis of the deformation behaviour of pure aluminium in repetitive corrugationstraightening and constrained groove pressing, 2018
- 76) Farhad Rahimi , Masoud Ahmadi, Bagher Mohammad Sadeghi, Finite element analysis of the deformation behaviour of pure aluminium in repetitive corrugationstraightening and constrained groove pressing, 2018